Available on CMS information server **CMS NOTE 1998/067**

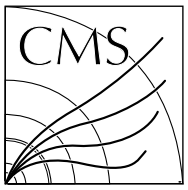

The Compact Muon Solenoid Experiment

CMS Note

Mailing address: CMS CERN, CH-1211 GENEVA 23, Switzerland

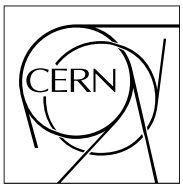

October 23, 1998

Activity of LUMEN (1996-97): understanding of $PbWO_4$ scintillator characteristics and their optimisation

S.Baccaro[1], P.Bohacek[2], B.Borgia[3], A.Cecilia[1], S.Croci[4], I.Dafinei[3], M.Diemoz[3], P.Fabeni[5], A. Festinesi[1], O. Jarolimek[6], E. Longo[3], M. Martini[4], E. Mihokova[2], M.Montecchi[1], M. Nikl[2], K. Nitsch[2], G.Organtini[7], G.P.Pazzi[5], G. Spinolo[4], A.Vedda[4]

INFN - Sezione di Roma

[1]*ENEA, INN-TEC, Casaccia, Roma (Italy)*
[2]*Institute of Physics, Academy of Science, Prague (Czech Republic)*
[3]*Dipartimento di Fisica, Università La Sapienza, Roma (Italy)*
[4]*INFM, Dipartimento Scienza dei Materiali, Univ. di Milano*
[5]*IROE-CNR, Firenze (Italy)*
[6]*CRYTUR, Turnov (Czech Republic)*
[7]*Dipartimento di Fisica, Universita' di "Roma TRE", Roma (Italy)*

Abstract

The aim of the LUMEN co-operation, supported by INFN, is to obtain full experimental characterisation and deep expertise of heavy scintillator for high energy physics. The advantage of this collaboration was mainly in the complementary character of the experimental techniques available in the partner laboratories and in the availability of highly experienced scientists in different fields. Furthermore close feedback to technological laboratories preparing "on request" PWO samples appeared extremely helpful. The present paper reports on the most important results obtained during the LUMEN activity in 1996-97. The aim of the report is to provide also enough useful information for the PWO application and novel ideas to stimulate further interest for new detectors as well as application in different fields.

FOREWORD

The CMS experiment (Compact Muon Solenoid), to be installed at the future Large Hadron Collider (LHC) at CERN, is proposing the construction of a scintillator based high resolution homogeneous electromagnetic calorimeter. An ideal calorimeter for High Energy Physics requires a dense, fast and radioactive hard scintillator. After a systematic investigation, the CMS-ECAL (Electromagnetic Calorimeter) collaboration finally has chosen Lead Tungstate ($PbWO_4$) crystals.

An international co-operation among technology and physics laboratories is necessary to optimise the $PbWO_4$ scintillation properties for LHC application and to ensure its reliability in mass production. Indeed full characterisation of PWO scintillator for LHC application includes comprehensive measurements of light transmittance, light yield, luminescence and scintillation properties at room and low temperatures, thermostimulated luminescence and thermostimulated currents and eventually radiation resistance.

These considerations provided the stimulus for the LUMEN co-operation: the aim was and is to obtain full experimental characterisation and deep expertise of heavy scintillator for high energy physics. The advantage of this collaboration was mainly in the complementary character of the experimental techniques available in the partner laboratories and in the availability of highly experienced scientists in different fields. Furthermore close feedback to technological laboratories preparing “on request” PWO samples appeared extremely helpful.

At the beginning, the collaboration was based among INFN (Sez. di Roma), ENEA (Dip. Innovazione), Dip. Scienze dei Materiali (University of Milan), IROE-CNR Firenze and Institute of Physics, Prague (Czech Republic). During the second part of 1996 we began a fruitful collaboration with Japanese laboratories, in particular with Prof. Kobayashi from KEK-IPNS (Tsukuba), Dr. M. Ishii from Shonan Institute of Technology (Fujisawa) and Dr. Y. Usuki from Furukawa Co. (Iwaki). Obviously, this activity is strongly related to CERN group involved in CMS-ECAL collaboration, especially with Dr. P. Lecoq and Dr. E. Auffray, mainly for measurements of crystals grown in Bogoroditsk. Last year we performed also measurements in collaboration with Dr. M. Korzhik and Dr. A. Borisevich from the Institute for Nuclear Problems (Minsk), to optimise the crystal of Russian production.

It will be no surprise that this report on the PWO properties does not provide a complete coverage of this field but an overview of our most important results obtained in various collaborations. The aim of this report is to provide also enough useful information for the PWO application and novel ideas to stimulate further interest for new detectors as well as application in different fields.

We are grateful to INFN for its full support and we thank the authors for their contributes.

Stefania Baccaro
(Lumen coordinator)

1 Introduction

The single crystals of $PbWO_4$ (PWO) became subject of increased interest in the nineties, because of their potential usage in detectors for High Energy Physics (HEP) experiments, namely in their electromagnetic calorimeter parts as a scintillation material. Essential luminescence characteristics of PWO are known for quite a time [1,2,3] as well as reports dealing with the growth of tungstate and molybdate single crystal systems [4,5], but first systematic scintillation studies appear few years ago [6,7,8] revealing its potential just for HEP field. Starting from 1994 rather systematic investigation effort as for PWO scintillation characteristics has started, because of its choice for electromagnetic calorimeter within CMS detector in LHC experiment in CERN.

It is well established that PWO emission spectrum consists of two emission components, the blue one peaking around 420 nm (2.9 eV) ascribed to the regular lattice center, namely $(WO_4)^{2-}$ one [1], and the green one peaking round 480 - 520 nm (~2.5 eV) ascribed to a defect center WO_3 [2]. In recent studies, several new facts came out, namely the existence of (at least) two different emission centers in the green spectral region. Apart from WO_3, Mo impurity, (i.e. the $(MoO_4)^{2-}$ group) is related to the component around 520 nm [9,10]. Speculations appeared as for possible local wolframit-like distortions of (scheelite) PWO lattice and their relation to the PWO green emission [11,12] as well as another super-ordered phase in (lead and oxygen deficient) PWO lattice was reported, namely $Pb_7W_8O_{32-x}$ (x=2.8) [13] and its possible role in green emission mechanism was discussed as well [14]. In the blue emission component, possible involvement of Pb^{2+} excite state levels was proposed even in the relaxed excited state [15] and two different decay kinetics mechanisms have been reported as well [16]. Rather complicated "spread-eagle" shape of this component observed clearly at 4.2 K was explained by the influence of Jahn-Teller effect on the degenerated excited state of WO_4 tetrahedron [17].

Decay kinetics of the blue and green emission components has been described already in [1] using a three-level-excited-state model to explain observed temperature dependencies. Recently, more complicated behaviour in the decay kinetics mechanism was observed, namely very slow non exponential components have been observed even under selective excitation within the lowest absorption peak of PWO above some 180 K [18], namely in the green part of spectra both in photoluminescence and scintillation decays. Recently, it was proved by measuring excitation spectra of thermoluminescence [19] that thermally induced decomposition of the excited state of both the blue and green emission centers takes place above some 150 K, which establish an intrinsic equilibrium between the bound (excitonic) states and free electron-hole charge carriers in conduction and valence bands, respectively. This essential result can explain the coexistence of the 1^{st} and 2^{nd} order decay mechanisms observed clearly in the decay under low repetition rate laser excitation [18, 20], as well as the "three-exponential character" of the scintillation decay reported by several groups [6-10].

Because of the intrinsic role of free charge carriers in the energy transfer processes in PWO lattice above 180 K, any shallow trap states in PWO lattice taking part in carrier capture processes become important, because they may modify strongly the diffusion rate of free charge carriers and consequently the speed of radiation recombination based on recombination of (originally) free electron and holes re-captured at emission centers. Such trap states are often efficiently monitored by thermoluminescence (TSL) measurements after irradiation at low temperatures. TSL measurements have been already reported a time ago [21] and also recent measurements confirm the rich variety of such shallow trap states in PWO lattice [22-25]. A strong correlation was found between the intensity of TSL peaks in the 150-300 K region and the presence of slow tails in luminescence decay [20], confirming the role of trap states in decay mechanisms. Measuring also TSL emission spectra, an important fact was found, namely that at the glow curve peaks at the lowest temperatures (from some 30 K until about 120 K), the emission is at least partly composed from the blue emission component [24,25], which can be most probably explained by (auto)-localisation of at least one of free charge carriers in regular PWO lattice at these temperatures. It is worth to note that such processes have been noticed also in another ternary oxides, e.g. $LiTaO_3$ [26] or $LiNbO_3$ [27]. On the contrary, green and red emission within TSL glow peaks above 180 or 300 K, respectively, evidences the processes of carrier capture driven by defects [25].

The processes of radiation damage and following recovery are of special attention, because resulting loss of transmission, instability of light yield (LY) or even induced changes in the scintillation mechanism can strictly limit the applicability of a scintillator material in a radiation severe environment of planned detectors

in HEP experiments. Systematic measurements of transmission changes on many PWO big crystal segments [28] revealed at least three categories of crystals based on the transmission curve of as grown crystals and related three crystal categories with respect to the radiation induced absorption behaviour. In general, it is known that the presence of any absorption band below a transmission cut-off (i.e. in the spectral region where the crystal should be transparent) and/or extended slowly decreasing absorption in this region indicates the presence of traps, which might create even deep trap states taking part in radiation damage processes at room temperature. The presence of two such absorption bands around 350 and 420 nm was established in the transmission of as grown crystals and 420 nm band was ascribed to O^- hole centers [29], while 350 and 420 nm bands were ascribed to O^- and Pb^{3+} hole centers, respectively, by another authors [30]. The recovery processes monitored at different wavelengths of induced absorption spectra have shown non-trivial decays well represented by two (three) exponentials showing the decay times of few hours until several days [28].

Also annealing PWO samples in different atmospheres and induced changes in the transmission spectra were employed to further study the optical properties of defect centers in this material. Studies were focused e.g. on the nature of 420 nm absorption band, which was noticed in transmission spectra already some time ago [4, 7] as well as in recent samples [28] and was recognised as one reason for lower LY in full-size PWO segments, because of its perfect overlap with the fast blue scintillation component of PWO and resulting re-absorption losses. Annealing induced absorption in 420 nm band was increasing under annealing in air (oxygen rich) atmosphere, while it was lowered after annealing in vacuum. In both cases, annealing temperatures in the range 600 - 900 ^{0}C were employed [29].

Presented overlook of earlier and recently reported results related to PWO emission and scintillator characteristics illustrates well the complexity of this material and the sometimes contradictory results reported by different laboratories. It is the aim of LUMEN collaboration, which was based in the first half of 1996, to continue in the research related to the understanding of the scintillation and radiation damage mechanisms of PWO, which had been carried out before in some of the participating laboratories and to propose possible ways leading to the material improvement to meet the demands of mentioned CMS application.

2 Experimental techniques in participating laboratories

The results have been obtained using several different techniques [30]. Emission and excitation spectra were measured by Spectrofluorometer 199S (Edinburgh Instrument) in Institute of Physics, AS CR, Prague using steady-state hydrogen flashlamp and Philips 2233 photomultiplier (PMT) in photon counting mode. The same set-up was used for photoluminescence decay measurements in ns - μs time scale using ns-pulse hydrogen (or nitrogen) filled coaxial flashlamp coupled with the single photon counting detection method, which allows to monitor the decay times down to ~ 0.5 ns, see also [17, 18, 19]. However, high repetition rate of the flashlamp (typ. 20 - 40 kHz) is disadvantageous in the case, when the slow components cause overlapping of the decay curves with the tail(s) of preceding one(s), lower the dynamical resolution and change the shape of the decay measured. As such situation was found in PWO [18], excimer laser excitation by 308 nm XeCl line (FWHM ≈ 10 ns) and low repetition frequency (~ 10 Hz) was used and the decay was detected by a PMT (Hamamatsu R1398) in current regime and by a digital scope Tektronix 2440 in the optical laboratory of IROE del CNR, Firenze. Special technique used for PMT signal measurement in several time and sensitivity ranges followed by pasting these measurements together into a single decay curve allows to monitor the decay in a very extended time scale (10^{-9} - 10^{-3} s) and with high dynamic resolution up to 5 orders in magnitude [18, 20]. Scintillation decays were measured by classical single photon counting method with ^{22}Na radioisotope excitation in collaboration with CERN laboratory, see e.g. [18], later on this technique was installed in Prague laboratory as well.

In the Dept. of Material Science, University of Milano, thermoluminescence techniques were used for the glow curves measurements to monitor the trapping states involved in the processes of radiative recombination of electrons and holes. Two different set-up's were employed. For low temperature TSL characteristics, a nitrogen cryostat was used and initial irradiation by an X-ray tube was performed at 90 K, followed by temperature sweep in 90 - 300 K range [20]. Repeated sweeps with several interference filters should be performed to obtain information about the spectral composition of the TSL signal [25]. The second configuration consists of irradiation at room temperature (RT) by X-ray or a radio-isotope (^{90}Sr-^{90}Y) and temperature sweep up to 800 K. In this case, besides usual detection performed by a photomultiplier, also

wavelength resolved TSL spectra could be obtained by a TSL spectrometer featuring a double stage microchannel plate followed by a diode array [25].

Light yield measurements were performed in the laboratory of INFN Sez. di Roma, by means of ^{22}Na tagging technique and other radioisotope sources [31].

The experiments related to radiation damage of PWO and annealing induced absorption changes are carried out in ENEA, Casaccia laboratory. Such experiment consists usually of the measurement of the transmission spectrum before and after an irradiation (or annealing) procedure and calculating the induced absorption coefficient $\mu(\lambda) = 1/d \log[T_0/T_1]$, where d stands for sample thickness and T_0 and T_1 are the trasmissions before and after irradiation (or annealing) procedure. As an irradiation source, the Calliope plant (Co^{60}) is used and transmission can be measured within 8 min after an irradiation procedure using a Perkin Elmer spectrophotometer. This spectrophotometer was completed also by an external optical path to allow measurements of transmission of full-size PWO segments (23 cm length). The Carbolite RHF 17/10E furnace and turbomolecular pumping station are used for annealing procedures allowing fully automatic control of the annealing temperature and vacuum atmosphere (if needed) .

Technological support of the LUMEN project is based on three crystal growth laboratories. The CRYTUR Preciosa a.s. (Turnov, Czech Republic) is a crystal growth company with long tradition in growing e.g. NaI, BGO, YAG, YAP, CeF_3 etc. crystals also doped with different ions essentially used as scintillator and laser materials. Research programme on PWO, started here in 1994, is based on Czochralski method in air atmosphere. The crystals of PWO up to 15 cm length, undoped and Nb, La, Lu, Y doped have been purchased in 96-97 period, which were grown from 4-5N raw material with dominant contamination by Mo ions at the level 10-15 ppm in a crystal. PWO samples from 5N purity raw material were grown in chemical dept. of Institute of Physics, Prague in close collaboration with CRYTUR using Czochralski method in controlled atmosphere. Undoped and La,Lu,Y and Gd doped samples have been grown for LUMEN experiments in 96-97 period up to 5 cm crystal length. The third technological laboratory is based in Furukawa, Ltd., Iwaki, Japan and samples were obtained in the frame of a collaboration with Prof. Kobayashi, KEK, Dept. of Physics, Tsukuba, Japan. The samples were grown in air by Czochralski technique using the third crystallisation procedure [9]. Undoped, La and Gd-doped samples were tested, up to 10 cm length.

Extended examinations of PWO characteristics were performed also for selected sets of PWO samples chosen from CERN center and by collaboration with Dr. Korzhik, which were grown in Bogoroditsk techno-chemical plant in Russia. Several tens of crystals were examined in all the laboratories and here we report only the results related to the more significant cases.

The samples mentioned by the names throughout the text have the following characteristics: PWO1, PWO2 and PWO3 (PWO1472) are undoped samples grown in Prague, in Turnov and in Bogoroditsk, respectively. PWO4 is K-doped sample (5 ppm in the crystal) grown in Prague. Furthermore, two undoped (***Und1_jp***, ***Und2_jp***) and two La-doped PWO samples (***La1_jp*** and ***La2_jp*** with 80 ppm and 460 ppm of La in the crystal, respectively) grown by Furukawa, Japan and three samples (undoped ***Und1_cz*** and doped ***La1_cz*** and ***La2_cz*** with 55 ppm and 380-560 ppm of La in the crystal, respectively) grown in the Institute of Physics, Prague will be mentioned. Moreover, also undoped crystal (***Und_bg***) as well as a Nb-doped crystal (***Nb-bg***) and a La-doped crystal (***La_bg***) both with 60-80 ppm of dopant in the melt and grown by Bogoroditsk techno-chemical plant have been considered. Finally ***Gd1_cz*** is the Gd-doped PWO (200 ppm in the crystal) grown in Prague.

3 Experimental results and discussion

3.1 Emission and decay kinetics characteristics of $PbWO_4$

3.1.1 Emission spectra

Previous studies have shown that PWO samples showing high level of the green emission component (GC) are not suitable for the HEP application, because of intense very slow components in the emission decay [9,18]. As a consequence, only the samples with dominant blue emission component (BC) were of interest for further studies.

X-ray excited emission spectra of three “typical samples”, named PWO1, PWO2 and PWO3 are given in Fig.1, curves a,b,c), at RT.

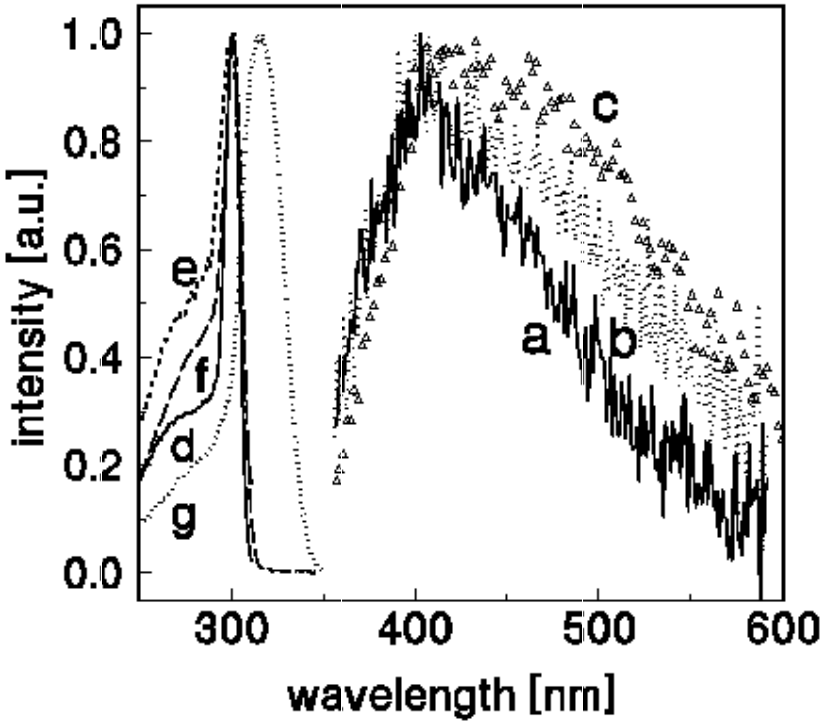

Figure 1: X-ray excited emission spectra of **PWO1** (curve a), **PWO2** (curve b) and **PWO3** (curve c) at RT. Excitation spectra at 80 K are given for **PWO1**, λem= 400 nm (curve d), λem = 500 nm (curve e) and **PWO2**, λem= 400 nm (curve f), λem= 500 nm (curve g).

Enhanced intensity in the green part of the PWO2&3 spectra evidences presence of the green emission component, which is actually given by the presence of mentioned Mo contamination at the level 10 - 15 ppm 45(PWO2) and WO_3 centers (PWO3). The fact that no (or negligible) amount of the GC is present in PWO1 spectrum can be derived from the absence of characteristic excitation peak at about 310 nm of the GC at 80 K, compare excitation spectra at λ_{em}=390 and 510 nm for PWO1, curves d),e) and PWO2, curves f),g), respectively. Further support can be obtained considering rather stable spectrum shape of PWO1 (under X-ray excitation) in 80 - 300 K range. Only minor changes in its shape are observed, which are probably induced by temperature dependence of Jahn-Teller effect related processes. Jahn-Teller effect influencing the degenerated excited state of $(WO4)^{2-}$ group was found responsible for complex "spread-eagle " shape of the BC emission spectra at the lowest temperatures [17]. Different temperature dependencies of the BC and GC emissions (mentioned already in [18]) result in rather distinct shape changes of overall emission spectrum especially in 200 - 300 K range.

Temperature dependencies of the blue and green emission components under X-ray excitation are given in Fig.2 in 80 - 300 K range for PWO1&2 samples.

The intensities of the BC and GC were obtained by calculating the area under the appropriate component spectrum at each temperature. In PWO2 sample, the blue and green components were separated by subtraction of suitably normalised PWO1 emission spectrum from the spectrum of PWO2. Such procedure assumes equal shape of the BC emission spectrum in both samples, which was confirmed at the lowest temperatures [17], being rather natural consequence of the fact that the regular lattice center is responsible for this emission component. The BC intensity was normalised in both PWO1 and PWO2 to 1 at 80 K (actually there is only small difference in the absolute BC intensity in both samples given by slight differences in the sample shape and uncertainty in the experiment geometry), which enables to follow and compare differences in their temperature dependencies.

Two consequences can be deduced from Fig.2:

i)The BC intensity is systematically lower in PWO2 above 180 K with respect to PWO1.

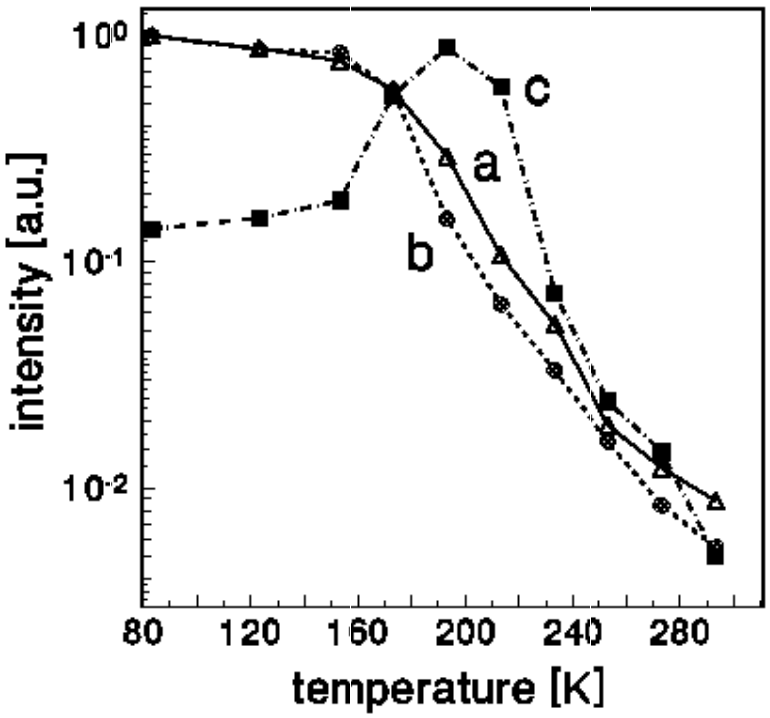

Figure 2: Temperature dependencies of the blue emission component (curve (a) for **PWO1**, curve (b) for **PWO2**) and the green component (curve (c) for **PWO2**) constructed from the emission spectra under X-ray excitation (see the text).

ii)The temperature dependence of the BC and GC intensities at T ∈ (150, 200) K can be explained just considering energy transfer from the BC to GC.

Emission spectra of La, Lu, Y and Gd doped PWO samples, properties of which will be discussed in the following paragraphs, do not show any changes with respect to the situation in Fig. 1 when grown from the same raw material and by the same technological sequence as undoped samples.

Emission spectra of Nb_bg samples show very low content of green emission at RT (noticeably lower with respect to PWO2), which becomes significant only around 200 K thanks to energy transfer processes mentioned above. The La_bg samples do not show any green emission at all similarly to the other trivalent ion-doped samples mentioned.

3.1.2 Decay kinetics

Decay kinetics of PWO was studied earlier by some of us in [18,19,20] and the co-existence of the decay of the 1st and 2nd order kinetics was evidenced in the blue emission decay as a result of mentioned thermal disintegration of the exciton excited state [19]. As a possibility for energy transfer between the BC and GC centers was noticed in the temperature dependencies of emission spectra (see 3.1.1) and the presence of trivalent dopants at Pb site were found highly useful for increasing the radiation resistance of PWO (see 3.2), the influence of these two aspects was followed in detail in the decay kinetics experiments.

To clarify the energy transfer mechanism the decay curves of the BC and GC were measured under selective excitation into the BC excitation peak -see Fig.3 for T=193 K. As one can see, there is no sign of rising edge in the GC decay, which could evidence any nonradiative resonant energy transfer between the excited states of the blue and green emission centers. Taking into account this result, the only explanation might consist of the energy transfer between these two emission bands via free carriers travelling through the conduction and valence bands as sketched in Fig.4. Such mechanism can be considered only thanks to thermally induced escape of electron from the excited state level to the conduction band (CB) (and hole to the valence band (VB)) at T > 150 K as evidenced in [19].

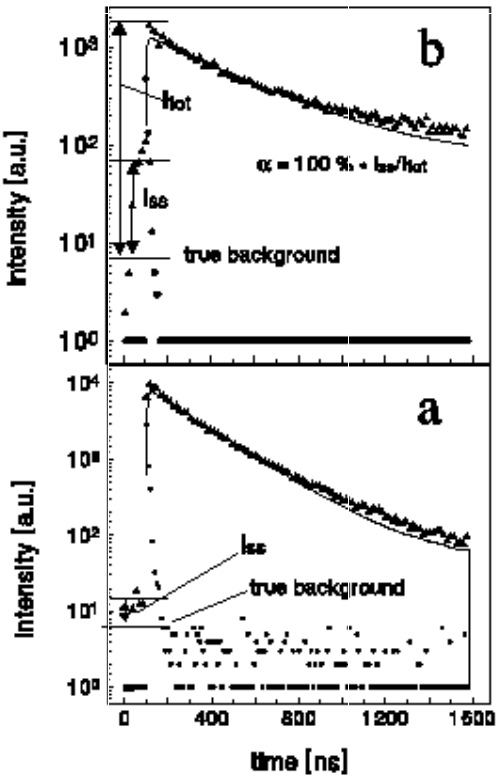

Figure 3: Photoluminescence decay curves for **PWO2** at 193 K excited by ns flashlamp (f_{exc} ~ 30 kHz). a) λexc= 305 nm, λem= 396 nm b) λexc = 305 nm, λem = 516 nm. The fit given by solid line is obtained by convolution of the instrumental response (also in the figure a) with a single exponential function showing the decay time 229 ns(a) and 392 ns(b). I_{SS} is the contribution to the background from the super-slow component.

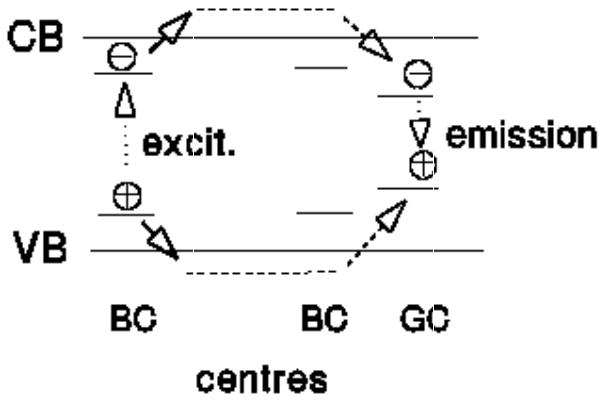

Figure 4: A sketch of energy transfer processes between the blue and green emission centers in $PbWO_4$ lattice (BC and GC stand for the blue and green emission centers, respectively).

Such relatively slow free charge carriers migration involved in the energy transfer process can not affect the rising parts of sub-microsecond decays at these temperatures, but it can be observed through the appearance of very slow (recombination) tails in emission component decays already noticed in [18]. Similarly to the approach given in [18], the coefficient α is defined in Fig. 3b, which appreciates quantitatively the presence of the decay components, which are slow with respect to the repetition frequency of the excitation flashlamp (≅ 30 kHz). Such components cause artificial increase of the "background" usually obtained from the signal level preceding the leading edge of photoluminescence decay. True background level can be obtained by running

the decay measurement in the same conditions, but e.g. with crossed excitation slits. Following the sketch in Fig. 3a,b, considerably high value of α is obtained in the green part of emission spectrum at 516 nm (α_{GC} = 3.7 %), while negligible value was found in the blue region of spectra at 396 nm (α_{BC} =0.05%). The reverse (GC to BC) energy transfer channel becomes effective probably at somewhat higher temperatures, which is in agreement with ref. [19] as well and this process is responsible for slower (even if weak) tails in the BC decay at T > 250 K. Bi-directional energy transfer between the BC and GC centers round RT is also supported by the very similar shape of excitation spectra round excitonic absorption peak round 310 nm [18]. In temperature dependence of the GC(PWO2) in Fig.2, curve (c), the reverse energy transfer is effectively masked by the intense quenching of both components above some 230 K.

Supporting arguments for the hypothesis about energy transfer between the BC and GC can be obtained from Fig. 5, where at RT the luminescence decays excited by low frequency excimer laser (308 nm) are reported for PWO1 and PWO3, which show the emission spectra according Fig. 1a and 1c,respectively.

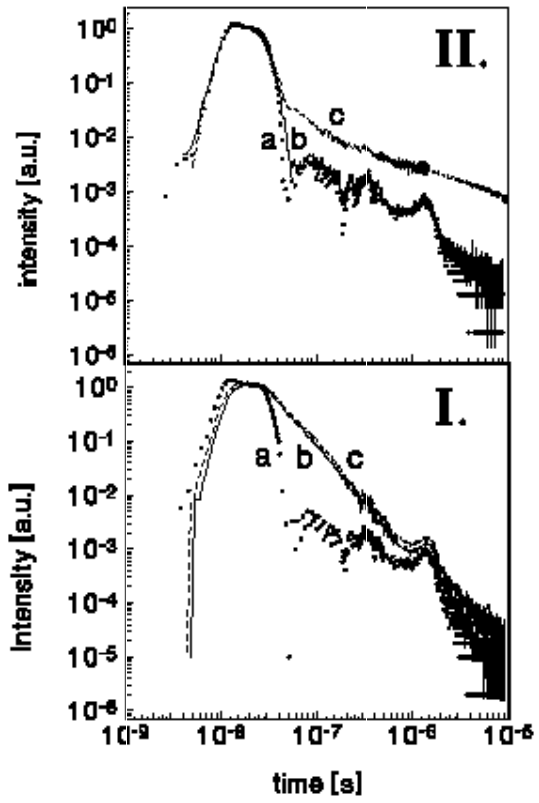

Figure 5: Photoluminescence decay curves at RT excited by excimer laser (XeCl line at 308 nm, f_{exc} ~ 10 Hz). I. sample **PWO1** a) laser pulse profile at 308 nm, b) λem= 400 nm, c) λem = 500 nm; II. sample **PWO3** a) laser pulse profile at 308 nm, b) λem= 400 nm, c) λem = 500 nm.

While the PWO1 (the BC only) shows rather similar decay course at 400 and 500 nm with strong recombination component, the PWO3 (spectrum with noticeable GC) show pronounced shortening of the decay at 400 nm, in which only the 1st order "immediate" decay component remains. On the other hand, very slow hyperbolic-like decay component is observed at 500 nm, which is clear evidence of the presence of slow 2nd order recombination processes. These energy transfer processes are discussed in detail in [33, 34].

In Fig.6 and Fig.7, strong effect of La^{3+} doping on photoluminescence (PL) and scintillation (SC) decays, respectively, is noticed in both 5N purity czech (Fig.6a) and japanese (Fig.6b) samples showing only the BC in the emission spectrum at 295 K (Fig. 1a).

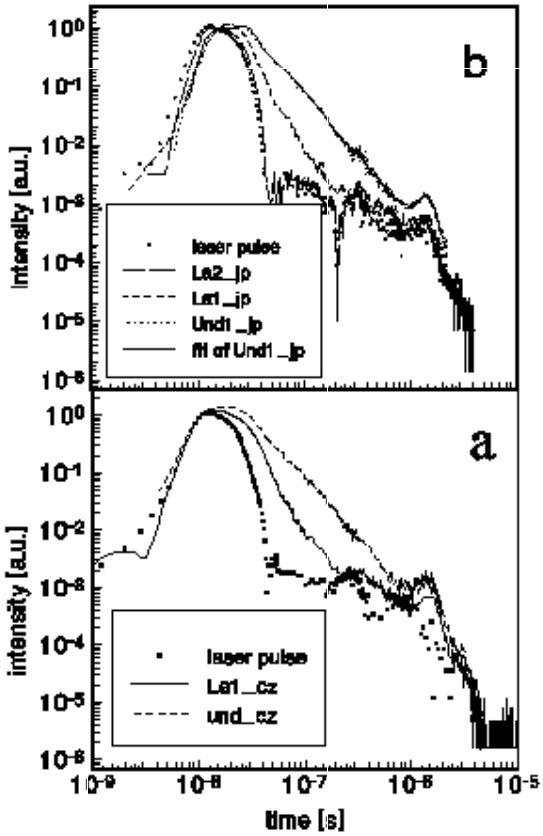

Figure 6: a)Photoluminescence decays of ***Und_cz, La1_cz*** samples and the instrumental response to the excitation laser pulse are given. b)Photoluminescence decays of ***Und1_jp, La1_jp, La2_jp*** samples and the instrumental response to the excitation laser pulse are given, the fit of ***Und1_jp*** by the sum of four exponentials ($\tau_{1,2,3,4}$= 1.6, 21, 63 and 266 ns) is also given by solid line. $\lambda_{exc.}$=308 nm (XeCl excimer laser line), $\lambda_{em.}$=400 nm and T=295 K.

Namely, the decay becomes shortened with increasing La concentration, because of diminishing recombination components. Due to their generally non-exponential course, only the mean lifetime τ_{mean} can be calculated. In the case of a multiexponential approximation of a decay curve $I(t)=\sum A_i \exp[-t/\tau_i]$, τ_{mean} can be calculated using the derived formula

$$\tau_{mean} = \frac{\sum A_i \tau_i^2}{\sum A_i \tau_i} \qquad (1)$$

Actually, the measured decays were approximated by the convolution of the instrumental response to excitation pulse and the above mentioned sum of 3-4 exponentials to obtain a true shape of the decay curve (the example of a fit is given in Fig.6b). The values of τ_{mean} were calculated - see Table I. Generally shorter values of τ_{mean} obtained for the SC decays with respect to the PL ones can be explained by the fact that in both cases the background level was determined simply from the signal level preceding the rising edge of the decay curve. Hence, in the SC decay, the contribution of the decay components, which are slow in comparison with "repetition frequency" of excitation 511 keV photons (about 30 kHz), was neglected. Relative amplitude of these “superslow” processes can be determined by the mentioned coefficient α, which is given in Table I. These results have been published recently in [35]. In Fig. 8, the photoluminescence of Russian La-doped and Nb doped PWO are displayed showing clear difference as for slow decay components above 10^{-6} s.

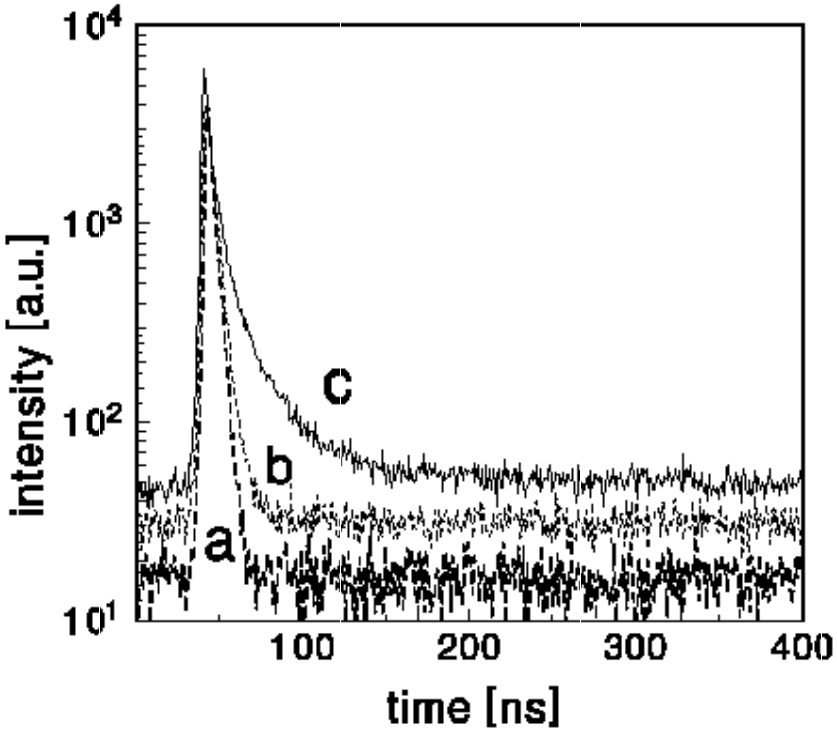

Figure 7: Spectrally unresolved scintillation decays of ***La2_jp*** (curve a), ***La1_jp*** (curve b) and ***Und1_jp*** (curve c). Curves are vertically shifted for better clarity. T= 295 K.

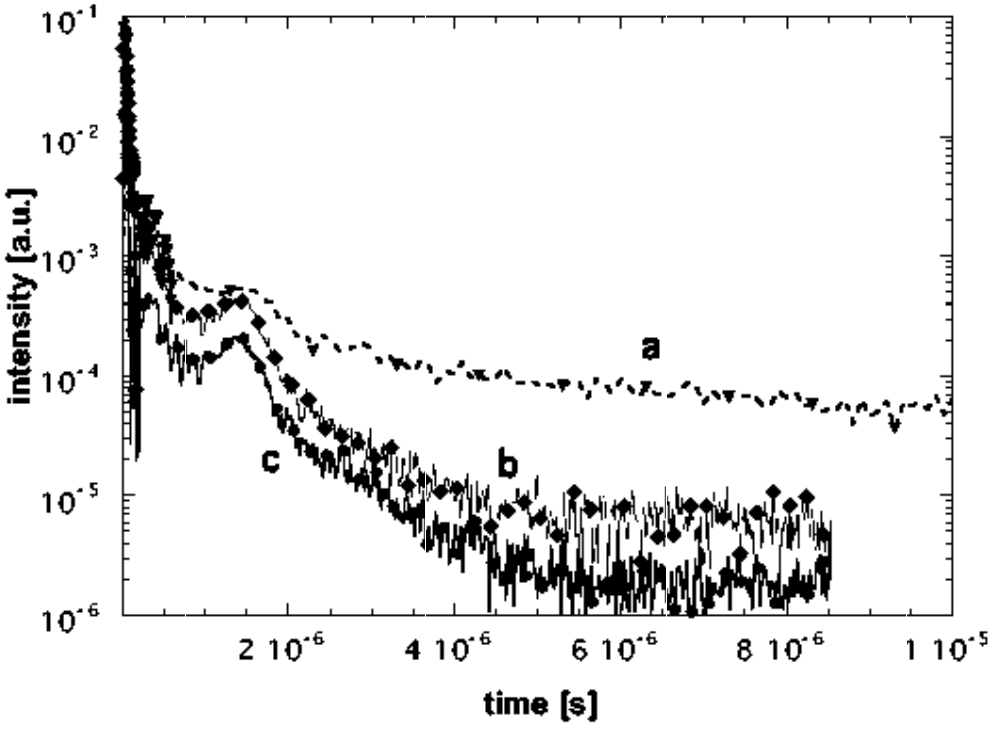

Figure 8: Slow tails in the photoluminescence decays at 500 nm of ***Nb_bg***, curve (a) and ***La_bg***, curve (b) are displayed at RT and under excimer laser excitation at 308 nm (XeCl line). Excitation pulse profile is given as well, curve (c).

Similarly to ***PWO2*** and ***PWO3*** samples, slow decay components are noticeable in ***Nb_bg*** ones, because of presence of green emission centers, while in ***La_bg*** ones these components are practically absent.

3.1.3 Thermoluminescence at low temperatures

As mentioned in the introduction, TSL measurements revealed a number of trap states evidenced through TSL glow peaks between 20 and 450 K [20-25]. As a negative impact of some of these trap centers on the speed of scintillation decay was recognised soon [20], the aim was to diminish their concentration and the doping by aliovalent impurities was investigated as one possible approach. As for the shallow traps related to the below-RT TSL peaks, the best results were achieved for stable trivalent dopants at Pb site (La, Lu, Y and Gd). The properties of PWO:La were investigated more systematically till now. In Fig.9, TSL glow curves are reported for the same samples as in Figs. 6 and 7. In spite of big differences among TSL characteristics of the samples in Fig.9, one can see that the presence of La^{3+} ions reduces strongly TSL peaks above 150 K.

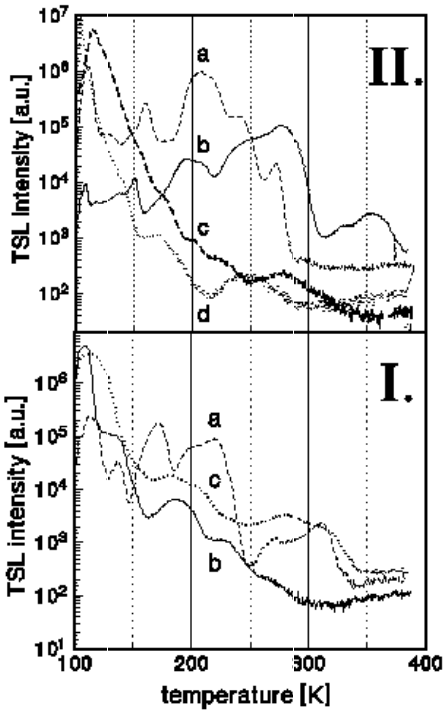

Figure 9: TSL glow curves (spectrally unresolved) after irradiation by X-rays at 90 K. I. Samples ***Und_cz*** (curve a), ***La1_cz*** (curve b) and ***La2_cz*** (curve c).II. Samples ***Und2_jp*** (curve a), ***Und1_jp*** (curve b),***La1_jp*** (curve c) and ***La2_jp*** (curve d).

At the same time, TSL peaks in the region 110-130 K are strongly enhanced, although a precise evaluation of their intensities is prevented in these measurements, due to i) close proximity between irradiation temperature and temperature at which the glow peak occurs; ii) possible non-linearity of the detection system in the presence of very high signals. The high intensity of 110-130 K TSL structures could be explained by taking into account either a concentration enhancement of the responsible defects, or the presence of competitive processes in carrier capture with traps related to 150 - 350 K peaks (the concentration of the latter traps being efficiently suppressed by La doping). The latter explanation seems to be more probable, if one takes into account the behaviour of calculated integrals of TSL signal in the range 100 -150 K and 150 - 350 K in Table I. Close relation of the TSL peaks round 180-220 K and 250 K to point defects in PWO lattice has been stated already [20], while the peaks around 110-130 K are probably connected even with regular lattice, i.e. auto-localisation of at least one kind of free charge carriers. The latter ascription is supported by the presence of the blue emission component in the TSL spectrum round 110-130 K [25]. It was mentioned that e.g. autolocalized hole centers O^- were evidenced in regular $LiTaO_3$ lattice below 120 K (see ref. 26) or in $LiNbO_3$ as well (see ref. 27), while electrons are stored most probably in O vacancies [25, 36]. These results have been published recently in [35].

Similar behaviour was found also for Lu, Y and Gd doped samples, an example is given in Fig. 10 for ***Gd1_cz*** sample.

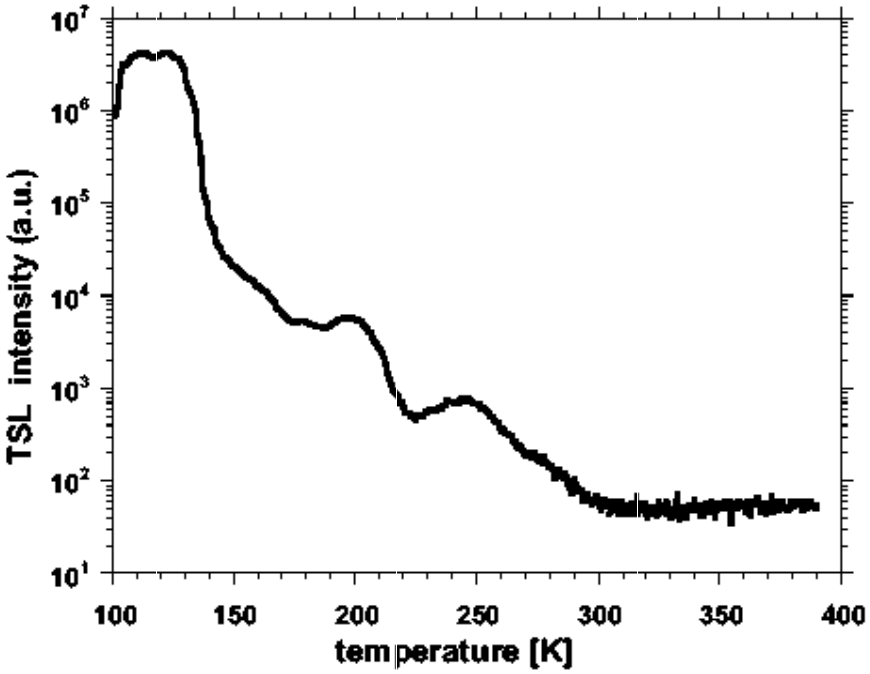

Figure 10: TSL glow curve (spectrally unresolved) for ***Gd1_cz*** sample after irradiation by X-ray at 90 K. (For equivalent, but undoped sample see curve I.a in Fig. 9)

On the contrary, Nb doped sample displays a high TSL intensity in the 150-300 K region, as shown in Fig. 11 where a comparison between ***Nb_bg*** and ***La_bg*** crystals is shown.

3.1.4 Light yield

There are essentially two different (limit) situations, in which the light yield (LY) of PWO is worth to be measured:

a) Small sample limit - minimum sample dimensions are restricted by the requirement to get reasonably high absorption of gamma-photons in the sample, i.e. well-defined photopeak The minimum volume is about 1x1x1 cm^3 for commonly used radioisotopes (^{22}Na, ^{60}Co, etc.). Scintillation light produced in such a small sample has rather high probability to reach the detector (low escape and re-absorption probability), so that such a measurement show an intrinsic LY limit of a sample material and is of help to determine the scintillation light production mechanism.

b) Full-size limit - related to the full-size segment for HEP application e.g. 2x2x23 cm. Additional escape and re-absorption losses lower the LY values measured with respect to an equivalent small sample. Optimisation of material as for the lowest possible absorption losses in the spectral region where scintillation spectrum occurs is of crucial importance. Such measurements are obviously important from the application point of view.

Systematic comparison of the LY values among La-doped and undoped PWO samples (the same set as in 3.1.2, 3.1.3) was made in a small sample limit, see [33, 35]. Correlation can be found between the fastening of the decay and LY decrease. It can be understood in the way that the recombination (i.e. free carrier based) processes are strongly suppressed in the case of high La concentrations, which probably create new "killer sites". At these sites effective non-radiative recombination of free electrons and hole occur (possibly close to La-dimers or La-small aggregates). Such a process inevitably leads to strong lowering of LY, τ_{mean} and α parameters - see Table I.

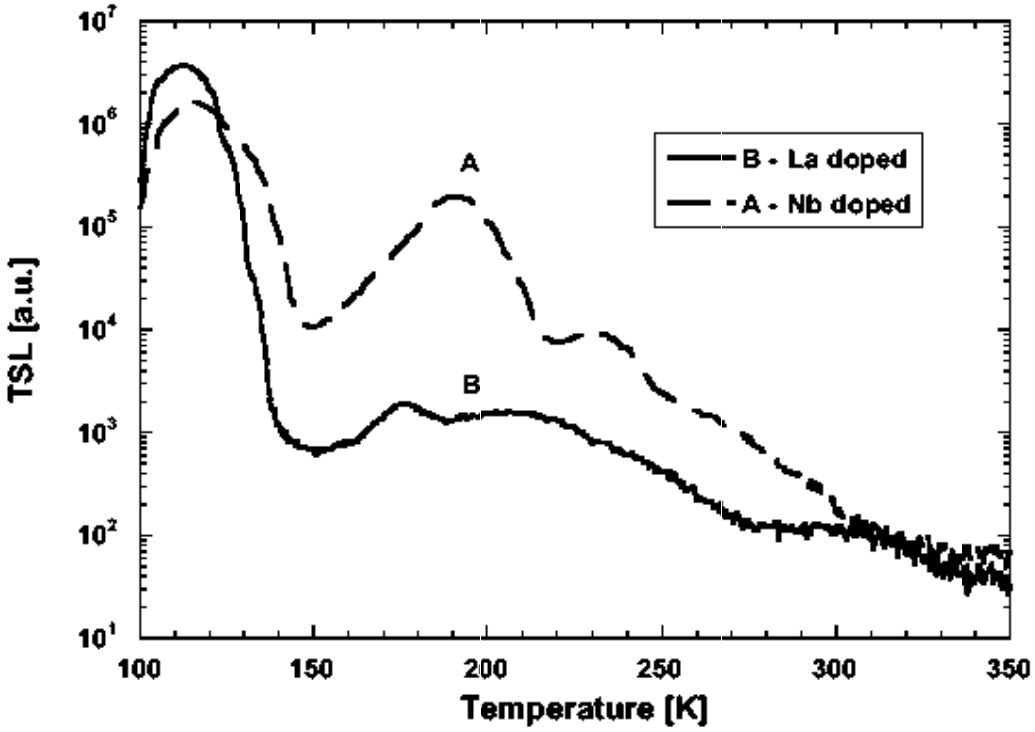

Figure 11: TSL glow curves of ***Nb_bg*** (A) and ***La_bg*** (B) samples following X irradiation at 90 K.

TABLE I. Calculated mean decay time τ_{mean} of the photoluminescence (λ_{em} = 400 nm) and scintillation (spectrally unresolved) decays using eq. (1), coefficient α related to the amplitude of the superslow decay components, integrals of the TSL glow curves in 100-150 K (I^{150}) and 100-300 K (I^{300}) intervals and light yield (LY) in 100 ns gate are given for all the PWO samples. The values of LY are measured at temperature t = 15±0.1 ^{0}C and normalised to t = 18 ^{0}C.

Sample	τ_{mean} **[ns] PL**	τ_{mean} **[ns] SC**	α **[%]**	I^{150}/I^{300} **TSL**	**LY phel/MeV**
Und1_jp	40.1	20.4	0.52	0.028/0.58	15.9±0.1
Und2_jp	34.4	21.1	0.67	1.2/4.4	16.5±0.1
La1_jp	9.3	3.7	0.43	8.2/8.3	11.1±0.2
La2_jp	2.2	2.4	0.17	3.9/3.9	4.0±0.5
Und1_cz	36.5	19.6	0.48	0.39/0.98	12.0±0.1
La1_cz	12.2	2.7	0.4	5.8/5.9	8.1±0.1
La2_cz	29.7	2.3	0.31	8.5/8.6	5.9±0.2
La_bg	25.0	-	-	11.2/11.3	8.5±0.5
Nb_bg	14/17870 measured at 500 nm	-	-	19.7/26.8	5.3±0.5

At intermediate La concentration, the effect of τ_{mean} shortening is much more pronounced than the decrease of LY: this fact can be interpreted in terms of a generally faster free carrier migration before radiative recombination. In other words, also in the case of the blue emission centers, the speed of radiative processes based on recombination of free carriers depends strongly on the presence of traps, which are efficiently

monitored by TSL measurements. These trap centers apparently capture temporarily free carriers at room temperature, which slow down their migration and consequently the recombination decay components become slower as well.

Observed LY values in Table I. (i.e. for the case of small samples showing negligible GC intensity) together with the knowledge of their PL and SC decays gives the possibility to estimate percentage of the "immediate" and "recombination" related scintillation light. It comes out that very fast immediate component (about 2-3 ns decay time at RT) contribute about 20-30% into the LY observed, while the rest is attributed to the delayed radiative recombination processes.

3.2 Radiation damage processes in $PbWO_4$

It is worth stressing that the initial stages of γ-ray induced radiation damage of PWO is essentially a three-step process consisting of (i) creation of hot electrons and holes by the interaction with high energy γ -quantum, (ii) their separation during subsequent cooling down and diffusion processes and (iii) separate localisation of both types of free carriers at suitable lattice sites (traps). Such sites might arise as a result of lattice distortions (dislocations, domain interfaces, etc.) or point defects (vacancies, impurity ions) or combinations of both of them. Colour centers might be created during (iii) as a result of a need for local re-creation of charge balance in the lattice (e.g. near to a monovalent or trivalent impurity ion at Pb^{2+} site in PWO, cationic and anionic vacancies, etc.). In case of PWO, one might expect in general the creation of F(two electrons in O vacancy), F^+(one electron in O vacancy), O^-, Pb^+ and Pb^{3+} centers. Most of these centers are paramagnetic and some of them have been detected in another scheelite tungstates by means of EPR, e.g. Pb^{3+} in $CaWO_4$ [37] and $(WO_4)^{3-}$ in several scheelites [38].

In general, no irreversible processes were observed during the irradiation of PWO up to high doses above 1000 Gy (e.g. formation of Pb colloids known from PbX_2 compounds), because the initial transmission of the samples was always restored by heating at 200 ^{0}C. This means that the stability of Pb^+ centers in the regular PWO lattice is strongly limited, because otherwise two electron capture in two steps at Pb^{2+} site becomes probable and subsequent creation of Pb^0 and Pb-colloids might follow as is seen in PbX_2 compounds mentioned.

3.2.1 Transmission of the as grown $PbWO_4$

Transmission of full-size 20-23 cm long PWO segments was systematically reported in [28] and the presence of 350 nm and 420 nm absorption bands was very clearly evidenced in many as grown samples. In [28] systematic diminishing of 350 nm band was noticed in Nb-doped crystals, while 420 nm absorption tended rather to increase after Nb doping. However, also in a few cm long undoped samples, these bands can be distinguished well - Fig. 12 (***Und1_jp*** and ***PWO4*** samples). These absorption bands clearly overlap scintillation spectrum of PWO, which has two negative consequences - lowering of LY in full-size samples and its inhomogenity along the segment as well. The doping by stable trivalent dopants at Pb site was found by us as very efficient tool in diminishing mainly 350 nm absorption band in as grown samples - Fig. 12 (***La1_jp*** sample), thus resulting in remarkable transmission improvement. These measurements were performed during the autumn of 96 in Casaccia and KEK laboratories using PWO:La produced in Japan and Czech Republic and published soon after [39, 40]. The effect was explained by the diminishing of hole centers concentrations (presumably ascribed to Pb^{3+} and O^- -like colour centers absorbing at 350 and 420 nm, respectively) by the excess coulombic charge of La^{3+} ions introduced into Pb sublattice.

Remarkable improvement of transmission achieved at 15 cm long CRYTUR La and Lu doped crystals is displayed in Fig. 13.

3.2.2 Gamma-irradiation induced absorption changes

Investigation of gamma-irradiation induced absorption is one of the most important characterisations in the case of PWO, because of planned applications in radiation severe environment. In this case rather systematic measurements at small sample set were performed in ENEA, Casaccia with the aim to understand microscopic processes in the color centers creation and their stabilisation in PWO lattice, for the details see [41].

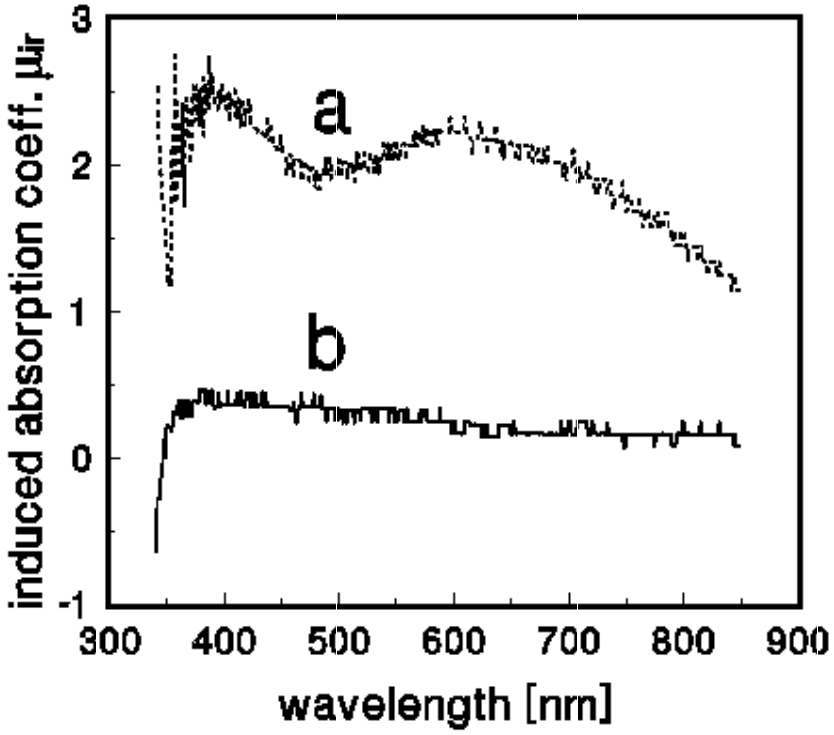

Figure 12: Room temperature transmission spectra of ***Und1_jp***, ***La1_jp*** and **PWO4** samples.

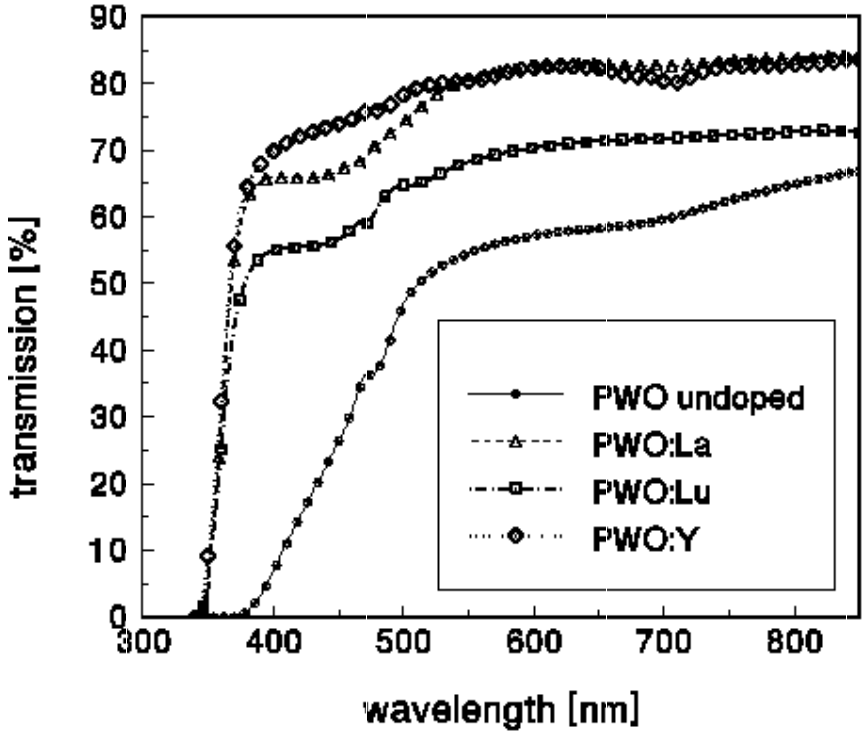

Figure 13: Transmission of 15 cm long PWO segments at RT, undoped, La, Y and Lu-doped.

PWO4 has shown the clearly structured μ_{ir} spectra at applied doses between 1 - 40 Gy - Fig.14, which, by itself, does not give a reasonable chance for unambiguous decomposition into gaussian curves

enabling ascription to some color centers afterwards. Hence, another procedure was applied in this case to induce the changes in its absorption spectrum in a different way, namely annealing in air and vacuum at high temperatures (see also 3.2.4). The sample as grown was subjected to subsequent annealing at about 950 ^{0}C for about 12 hours in air (oxygen rich) and low vacuum (oxygen poor) atmospheres. The resulting absorption spectra are given in Fig.15. The changes observed in the absorption spectra are stable even at temperatures above 200 ^{0}C unlike the irradiation induced spectra. This points to rather different mechanism of stabilisation for the annealing induced absorption centers. However, the centers themselves might be quite similar since we consider only centers arising as the result of free charge carrier capture (electron and holes) at suitable lattice sites. The annealing induced absorption coefficient μ_{an} after each procedure is given in the inset of Fig.15.

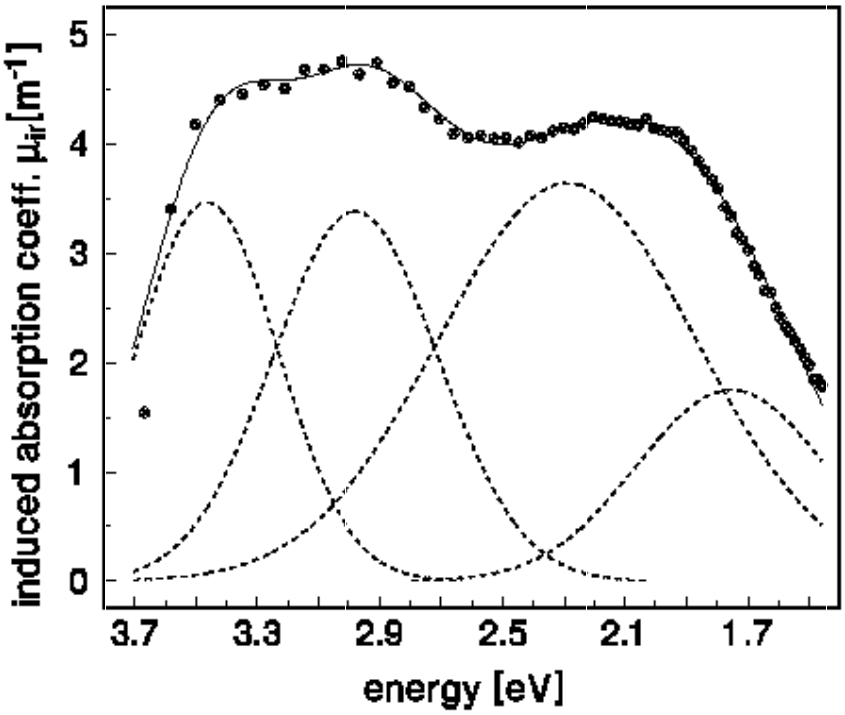

Figure 14: Induced absorption coefficient μ_{ir} spectra are given for **PWO4** sample and 41 Gy dose. Experimental curve is fitted by the sum of four gaussians (solid line, for the description see the text), separate gaussians (dashed line) are also given as an illustration.

Two absorption bands can be quite well resolved in the annealing induced absorption spectra in the inset of Fig.15 peaking at about 2.9 (~420 nm) and 3.5(~350 nm) eV.

On the basis of correlated increase and decrease of the 2.9 eV and the 3.55 eV induced absorption bands shown in the inset of Fig.15 and the fact that the 2.9 eV band is ascribed to the O^- hole center [29], the 3.55 eV band (observed also in the as grown crystals, see 3.2.1), might be ascribed also to a hole center, most probably the Pb^{3+} one. Taking into account the scheelite structure of PWO, the presence of K^+ ions at Pb^{2+} site might induce two defect configurations, namely K^+ - O^- and K^+ - O^{2-} - Pb^{3+} ones. Similar centers might be created even in undoped crystals close to Pb vacancies, the concentration of which may increase, because of possible "lead deficiency" resulting from formation of the Pb_2WO_5 phase in the rest of melt, in the evaporated layer inside the growing chamber and so on [42], when the "open" Czochralski growth method is used.

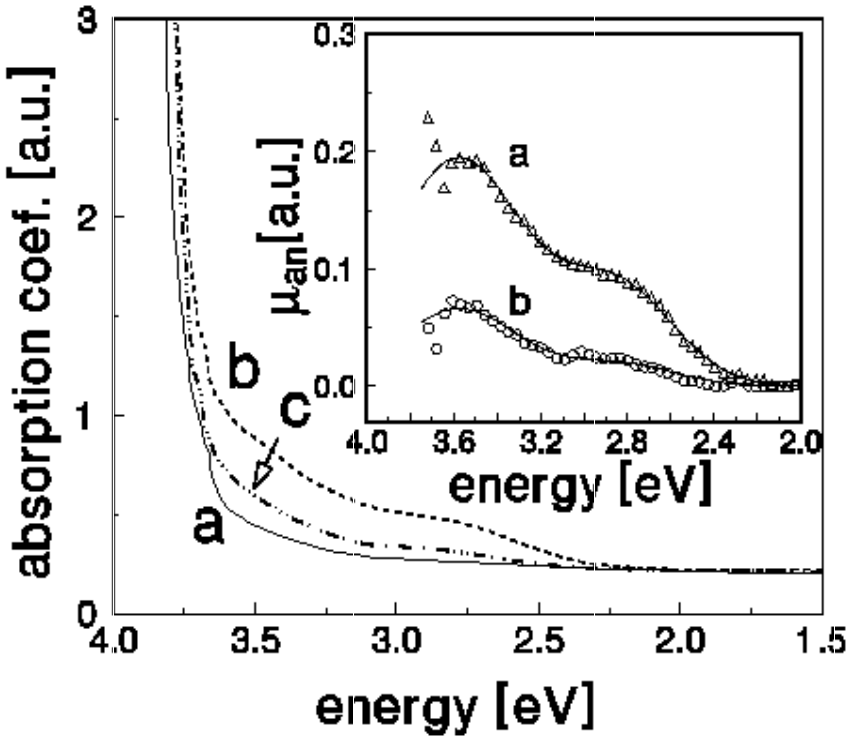

Figure 15: Absorption spectra of **PWO4** sample are given for the sample as received (a), after annealing in air (about 950 ^{0}C, 12 hours) (b) and after subsequent annealing in vacuum (about 950 ^{0}C, 12 hours) (c). In the inset, μ_{an} spectra are given for **PWO4** sample in air (a) and in vacuum (b). The μ_{an} is calculated relatively to the initial transmission before the first (in air) annealing procedure. Solid lines in the inset are obtained by fitting μ_{an} spectra by the sum of two gaussians peaking at 3.5 and 2.9 eV. Arbitrary units are used on y-axis, because the annealing induced changes are not homogeneous throughout the sample volume.

Taking into account possible position of the hole centers absorption obtained from annealing experiments above and position of absorption bands ascribed to F (520 nm) and F^+ (740 nm) electron centers [36] it makes sense to attempt the four gaussian fit of μ_{ir} with estimated maxima around 3.5, 2.9, 2.4 and 1.8 eV. One example of such a fit is given for PWO4 sample (41 Gy dose) in Fig.14, where μ_{ir} spectrum is fitted by the sum of four gaussians $\mu_{ir}(E)=\Sigma A_i \exp[-\Delta^2_i/(E-E_{0i})^2]$, with parameters E_{0i}= 3.46, 2.98, 2.29 and 1.75 eV, and Δ_i= 0.55, 0.63, 0.99 and 0.72 eV, i = 1, 2, 3, 4, respectively. The fit of induced absorption spectra by four gaussian composition (keeping position and half-width of the components approximately the same) is proved by the good results obtained for several samples and it indicates that just localised electrons and holes (i.e. color centers) are responsible for the induced absorption features. Possible differences may arise in the color centers (coulombic) stabilisation and other crystal field perturbations nearby, which afterwards can be responsible for observed scatter in the parameters obtained from fitting experimental data and differences in μ_{ir} spectra shape for different samples.

The above given interpretation as for the origin of the hole and electron centers has to be taken with caution, because there are no definite evidences given e.g. by EPR about their origin. Actually, till now the search for EPR resonances similar to those detected for Pb^{3+} centers in $CaWO_4$ [37] or $(WO_4)_2^{3-}$ [38] centers was unsuccessful. However, an explanation might be given by very recent electronical band calculations of Pb(Ca) tungstate and molybdenate structures [43], which show the substantial difference in the composition of the top of the valence band between Ca and Pb compounds. Namely, almost purely oxygen states form the top of valence band in Ca compounds, and considerable mixture between the oxygen and lead states is found in Pb compounds. As the top of valence band has a crucial role in forming the (defect-related) hole states, one could expect rather mixed Pb-O character of these states in PWO, while pure hole states were observed in (Pb-

doped) $CaWO_4$. The important issue however, which is addressed in [41] consists in the fact that there are (at least) two configuration of the hole states, which play important role in the radiation damage mechanism of PWO. It is also worth to note that stable existence of oxygen bi-vacancy up to some 600 ^{0}C was noticed in [44] for $CaWO_4$ after neutron irradiation. Such electron centers are not a priori excluded in PWO, e.g. the unknown "U1" centers in [45] show similar g-factors as bi-vacancy ones just mentioned. However, detailed temperature and angular dependencies are needed from coming EPR experiments to test such a possibility in detail.

Considerable improvement of radiation resistance was found for La doped small samples PWO, see Fig. 16 for the couple of equivalently grown undoped and La-doped japanese samples. Similar effect has been found for the crystal couples from three different technological laboratories [39], which evidenced general validity of this effect. Interesting effect was noticed in the dose dependence for some of these crystals, namely that above certain dose, the radiation damage of La-doped crystals was abruptly worsened - Fig. 17. The value of such a dose is clearly dependent on the origin of the La-doped crystals and at japanese samples, it did not show up even for the dose 10^6 Gy [46]. Positive effect of La doping was explained similarly as in the case of improvement of transmission, namely that excess coulombic charge introduced through trivalent ion at divalent lattice site reduces considerably the concentration of sites, which are able to localise temporarily holes created during irradiation. Dominant role of the hole centers in the radiation damage mechanism is based on the fact that hole charge carriers have shown much higher mobility in electrical conductivity measurements [47].

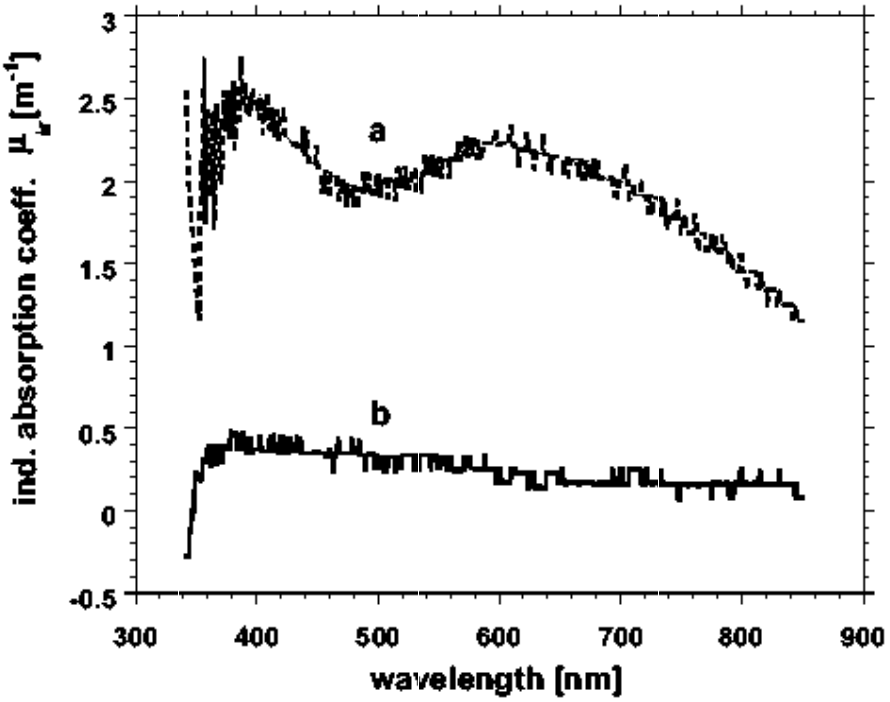

Figure 16: Room temperature induced absorption coefficient spectra (after 10 Gy dose) of ***Und1_jp*** (curve a), ***La1_jp*** (curve b) PWO crystals.

Six crystal samples of different crystallisation (Bogoroditsk convention) doped with La (3 samples) and with Nb (3 samples) were tested for their radiation hardness. The stronger UV shift of the fundamental absorption edge in the case of Nb doping was noticed for all samples (fig.18).

This result is confirmed by longitudinal transmission measurements made on full length CMS-ECAL (230 mm long) PWO crystals (fig. 19) [48]. The presence of the 420 nm absorption band visible in the case of full length crystals is hardly noticeable for samples only 14 mm long. Given the fact that only three samples each of a different crystallisation (1^{st}, 6^{th} and 9^{th} for La doped samples and 2^{nd}, 3^{rd} and 6^{th} for Nb doped samples) were available for each dopant it is difficult to extract a final conclusion regarding the influence of the order of crystallisation on the radiation hardness of the grown crystal. Nevertheless it is to be noticed the tendency of an lower radiation hardness of samples of higher order of crystallisation.

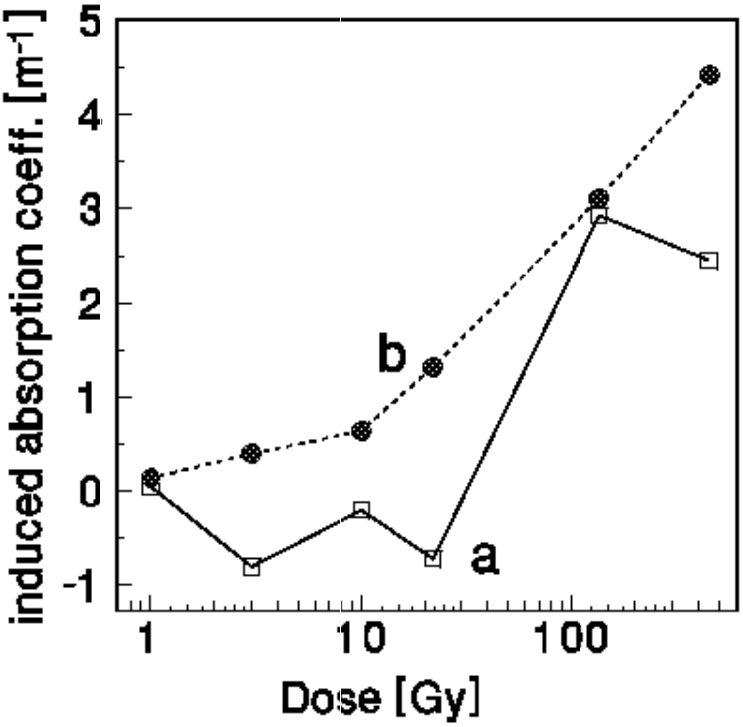

Figure17: Dependence of μ_{ir}(420 nm) (a) and μ_{ir}(520 nm) (b) on the irradiation dose for ***La1_cz*** sample.

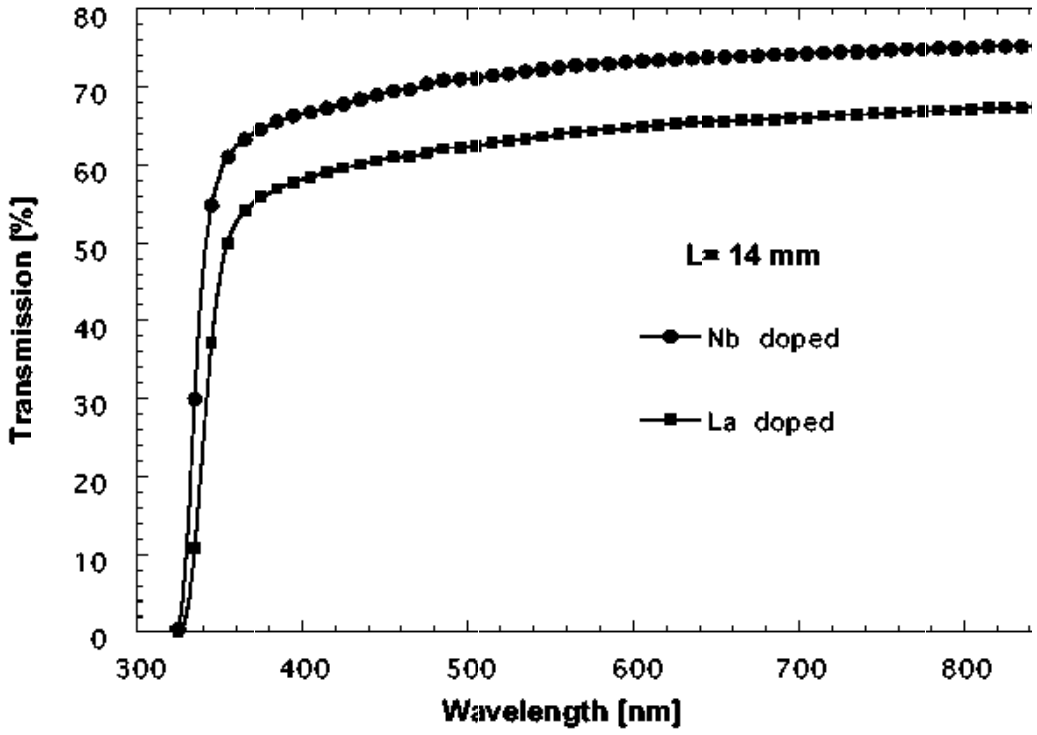

Figure18: Initial transmission of ***La_bg*** and ***Nb_bg*** samples of the 6th crystallization order.

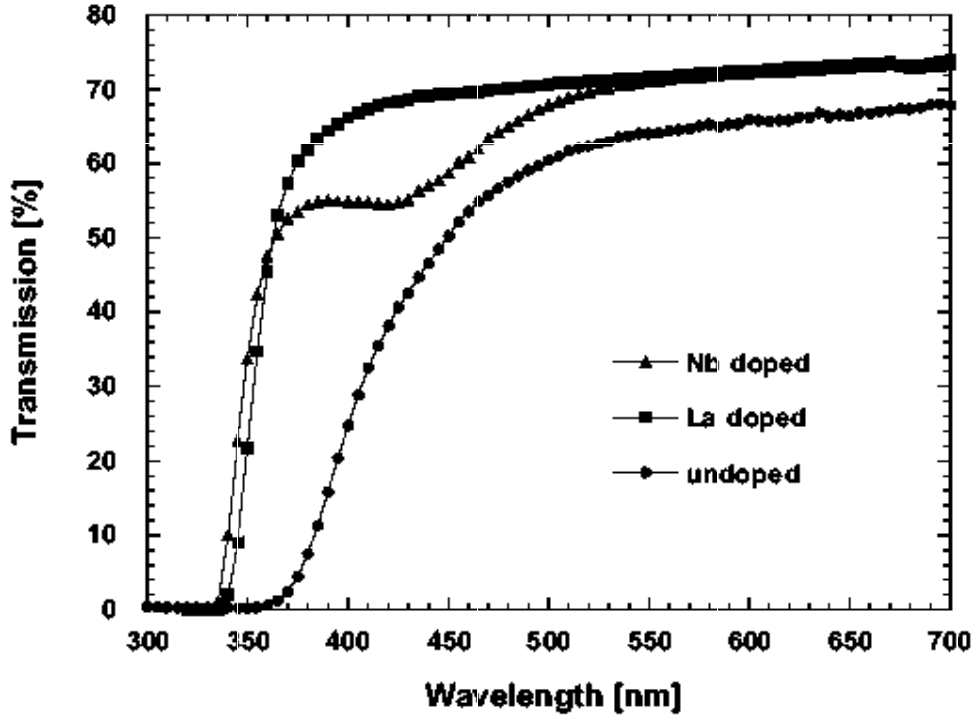

Figure19: Longitudinal transmission measurements ***Und_bg***, ***La_bg*** and ***Nb_bg*** samples (230 mm length)

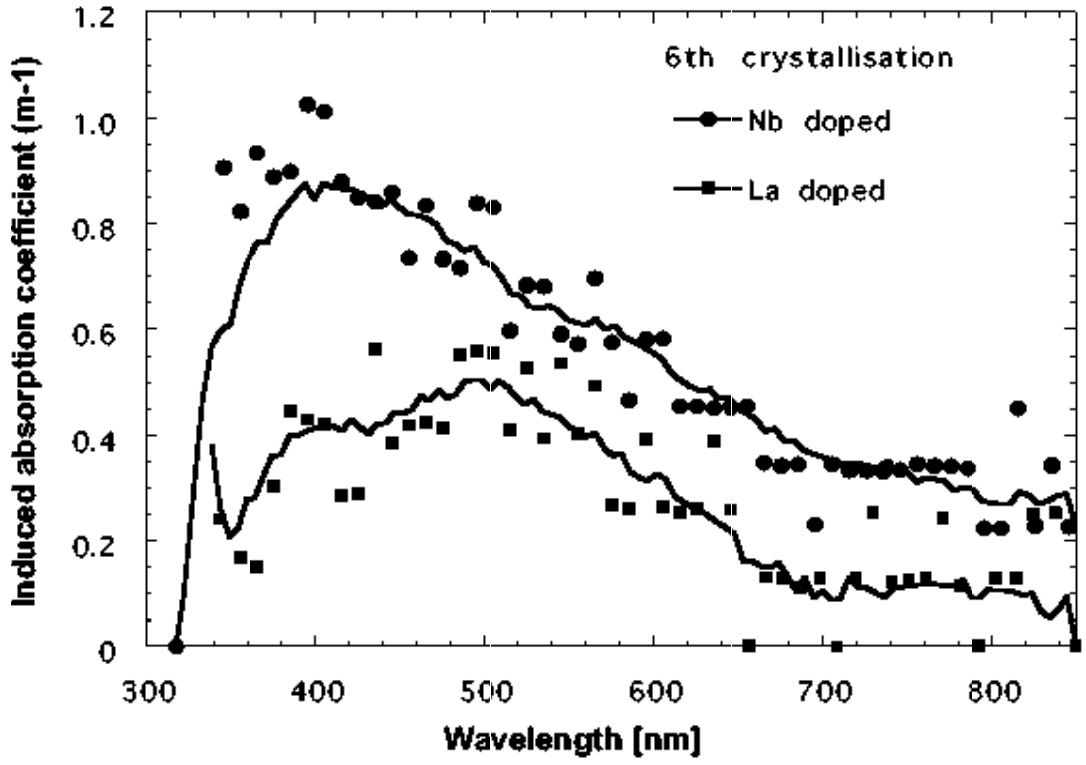

Figure 20: Radiation induced (30 Gy at 4.6Gy/h) absorption in ***La_bg*** and ***Nb_bg*** of the 6th crystallization order. The continuous line is the smoothed fit of experimental data.

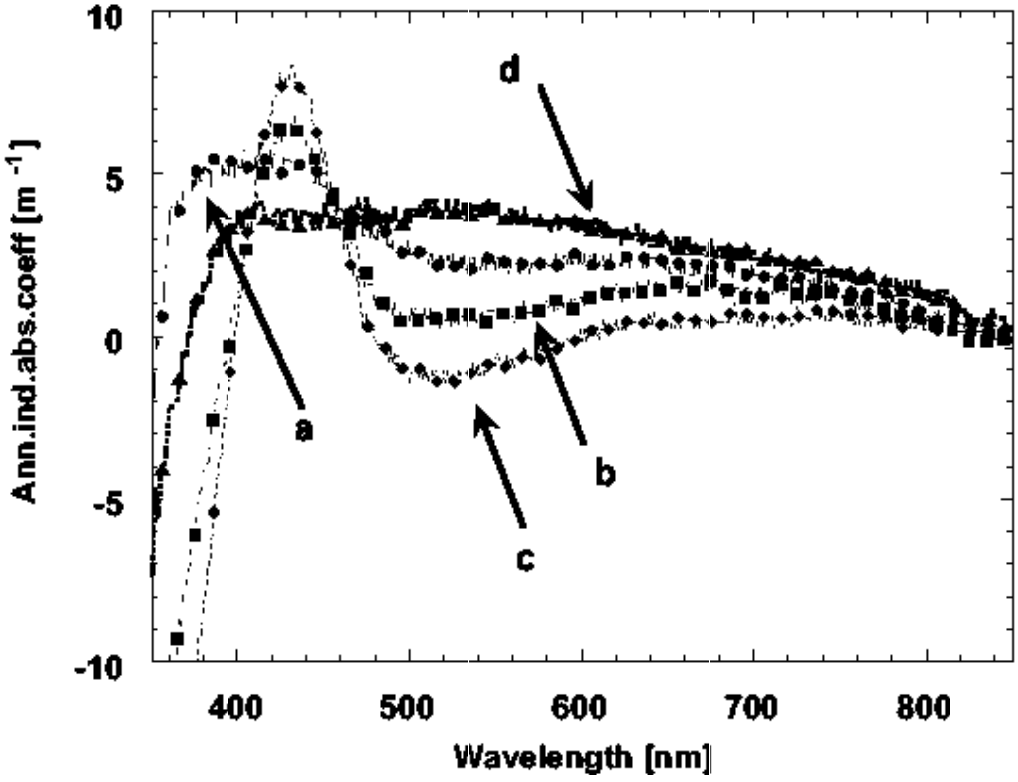

Figure 21: Annealing induced absorption in ***PWO1*** sample. The curves are given in the order as the thermal treatment has been made. (a) after annealing in air, 630 ^{0}C/12 hours; (b) after annealing in air, 850 ^{0}C/12 hours; (c) after annealing in air, 910 ^{0}C/12 hours; (d) after annealing in vacuum (10^{-5}torr) 590 ^{0}C/12 hours

More accurate tests are needed if one wants to decide which is the maximum number of crystallisation which still gives acceptable crystals from radiation hardness point of view. For samples having the same crystallisation order, the La doped have a higher radiation hardness that the Nb doped ones (fig.20).

Similar improvement of radiation hardness was found for Lu^{3+} and Y^{3+} doped PWO crystals [49, 50] and also for Gd^{3+} -doped ones [51], even if in this case the systematic studies have not been completed yet.

3.2.3 Neutron irradiation induced absorption changes

Investigation of radiation damage caused by fast neutrons has to be carried out as well, because of neutrons are produced in particle collisions in HEP colliders (e.g. planned LHC). In this case, the situation is more complicated: besides the production of color centers also irreversible processes due to other interaction mechanisms between penetrating neutrons and PWO lattice might occur. More, neutrons have pronounced ability to create radioactive isotopes in collisions with some lattice (impurity) ions resulting in increased radioactivity level of irradiated samples, which must be left some days after irradiation in irradiation chamber to avoid irradiation of the laboratory and working staff.

The CERN sample PWO 522 (10.3 mm length) was irradiated at reactor “Tapiro” in ENEA, Casaccia by neutron flux from 1.9 10^{10} - 4.72 10^{11} n/cm^2 and transmission changes and activation processes were tested. The observed transmission changes were within (relatively large) experimental error and no clear induced absorption structures were revealed [52].

3.2.4 Annealing induced absorption changes

Annealing of PWO crystals is adopted not only as a post-growth technological operation removing stresses etc. in PWO lattice, but also as a complementary experimental method allowing study of color centers production in a different way. The idea is that at sufficiently high temperatures (above 600 ^{0}C) , when mainly oxygen vacancies become mobile, the crystal can exchange oxygen ions with the environment. In oxygen rich

atmosphere, oxygen atoms can enter PWO lattice becoming O^{2-}, which should result in decrease of oxygen vacancy, F and F^+ electron center concentrations and increase of the hole (O^--like) ones under the assumption that such centers can be stabilised in PWO lattice. Conversely, in oxygen poor (close to vacuum) atmosphere, rather exiting oxygen atoms from PWO lattice are expected. A sequence of annealing procedures in the air and vacuum atmospheres at undoped 5N purity PWO crystal has shown that the behaviour of 420 nm induced absorption agrees with the above sketched trends for O^- centers, while another two absorption bands round 520 and 740 nm have shown opposite trends being thus logically attributed to the electron F and F^+ centers (Fig. 21) [36].

Similar annealing tests were performed also at Russian PWO samples [53]. Throughout extensive annealing tests of many different PWO samples the behaviour of 420 nm induced absorption band in these annealing experiments is one of the most reproducible phenomena among many other results in physics of PWO, which are often strongly technologically dependent.

3.2.5 Recovery processes at room temperature

The processes of spontaneous recovery of induced absorption at RT are related to the stability of radiation induced color centers, i.e. to the thermal depth of related trapping centers. They are studied to know the possibilities for bleaching damaged PWO crystals, if necessary, but also to appreciate the (in)stability of PWO parameters in the true working conditions in a calorimetric detector.

In Fig. 22, an example of the spontaneous recovery (in the dark at RT) of three PWO crystals 2x2x15 cm (undoped, La and Lu doped) is given after the dose of 450 Gy [48, 49]. It is evident that doping influences the thermal depth of the traps involved in the charge carriers capturing and their subsequent release. Such an effect has no immediate explanation, because a tight spatial correlation between the doped ions and traps can be hardly expected. On the other hand, it was recently found by EPR measurements that La-doping enhances cross section of electron trapping at MoO_4 centers in PWO [45].

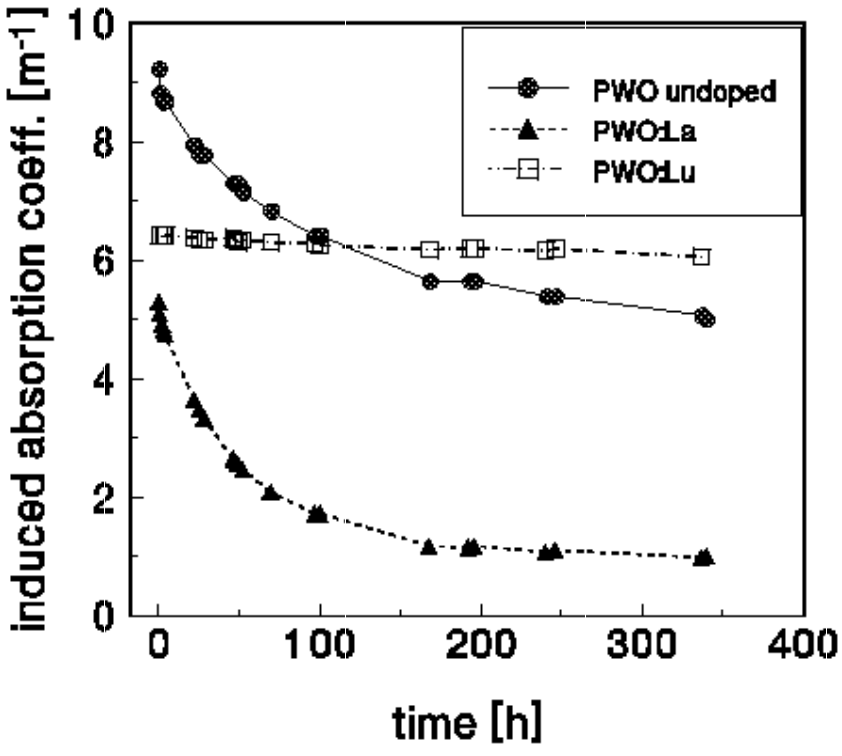

Figure 22: Recovery at room T of radiation damage in the dark for undoped, La and Lu-doped 2x2x15 cm long CRYTUR crystals after the dose of 450 Gy.

It was suggested that the depth of these electron traps is modified by coulombic potential changes in the space regions of PWO lattice, which contain La^{3+} ions, even if such an effect could arise also because of lack of

competition for electron capture (with respect to undoped sample).In this way one could propose that slight modification in coulombic potential arise when different trivalent ions are used (a second order effect, because of different charge distribution in space for different ions) and consequently the depth of electron traps is slightly different for various trivalent dopants

3.2.6 Thermoluminescence above room temperature

The trapping centers showing TSL glow peaks above room temperature are able to localise charge carriers even for rather long time (tens of hours), so that they can be directly related to the observed processes of radiation induced absorption. On the other hand, it is worth noting that above RT the processes of radiative recombination of free carriers (i.e. those observable through TSL) are often of minor importance (low intensity) with respect to extended possibilities of non-radiative recombination.

An example of the TSL glow curves above RT reported in Fig. 23 shows the presence of at least three different trap levels capturing free carriers during X-ray irradiation.

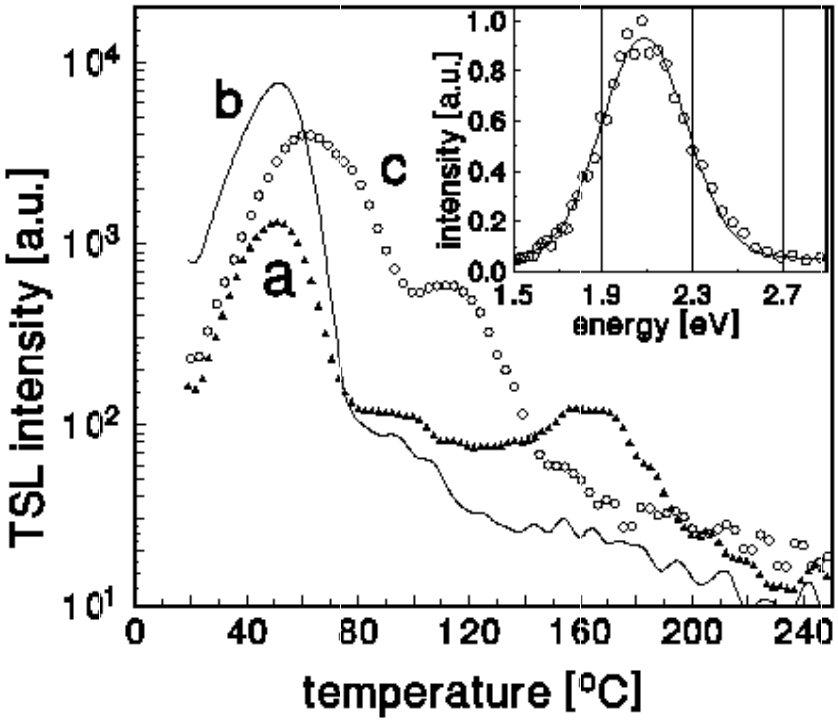

Figure 23: TSL glow curves are given for **PWO4** (a), ***Und2_jp*** (b), **PWO2** (c) samples after X-ray irradiation (10^4 Gy) at RT, heating rate 1 °C/s. In the inset, the TSL emission spectrum of the sample ***Und2_jp*** integrated in the 50 - 200 °C temperature range is also shown, fitted by a gaussian curve (solid line) centered at 2.1 eV.

The decay time of dominant 50 °C TSL peak (10 min at 293 K) does not correspond to rather stable amplitude of μ_{ir} within 10 - 60 min after irradiation [41]. This means that these TSL traps cannot be major centers related to the observed radiation induced absorption. On the contrary, a correspondence can be found between the decay times of the TSL traps related to the peaks at 100 and 160 °C and the recovery time of the absorption bands present in the μ_{ir} spectra [28, 41, 46]. Moreover, TSL traps are again completely emptied after a thermal treatment at 200 °C, after which treatment the radiation induced absorption spectrum is also completely bleached. This suggests that processes of radiative recombination could be involved in the overall complex mechanism of radiation damage recovery in PWO.

Also in the case of TSL above RT, significant effect was found after La-doping, namely TSL glow peaks above RT practically disappeared - Fig. 24.

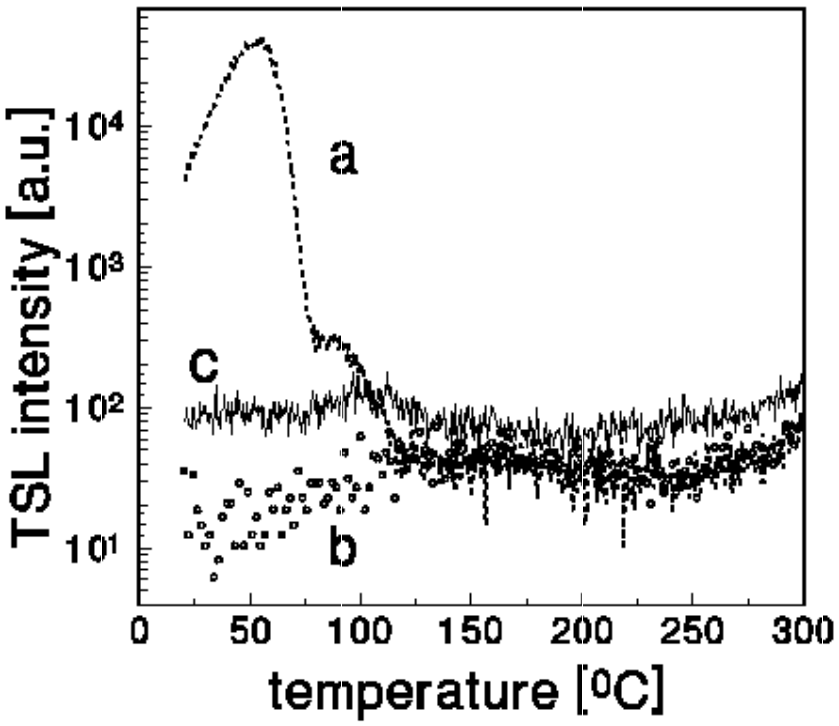

Figure 24: TSL glow curves are given for ***Und1_jp*** (a), ***La1_jp*** (b) and ***Gd1_cz*** (c) samples after X-ray irradiation (10^4 Gy) at RT, heating rate 1 ^{0}C/s.

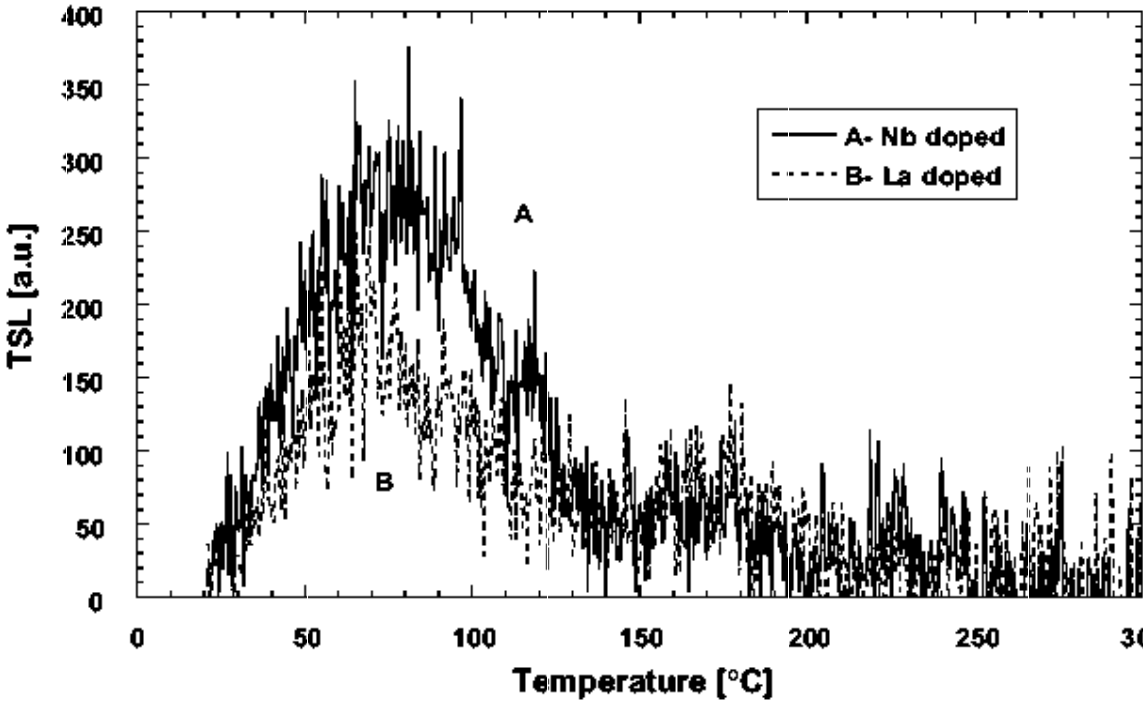

Figure 25: TSL glow curves of ***Nb_bg*** and ***La_bg*** following X irradiation at room temperature.

The most pronounced effect is observed for dominant TSL peak at around 50 ^{0}C. At variance with what observed in the TSL at low temperatures, also ***Nb_bg*** sample displays a weak TSL signal above room temperature similar to that of ***La_bg*** sample, see Fig. 25.

The TSL emission is in above-RT glow peaks centered at 2.1 eV (inset of Fig. 23) and is similar to so called "red luminescence", which was already observed in as grown PWO [8] and ascribed to Pb^{3+} centers. Such centers might be in principle responsible for the observed TSL emission; they act most probably as electron traps. It is worth mentioning the correlation of the intensity of TSL peak at 50 ^{0}C, the amplitude of the absorption around 3.5 eV (ascribed to Pb^{3+}) in the as grown crystals and the amplitude of μ_{ir} spectra, which was found several times for different sets of PWO samples. This correlation should be understood in the sense that there is some common origin (mechanism) of the creation of all these centers, even if they are not the same, which is clearly seen e.g. in different decay times in TSL and μ_{ir} spectra as mentioned above.

The absence of higher energy emission bands observed at low temperature TSL glow peaks can be explained by efficient thermal quenching of these bands above RT and/or by inefficient capturing of free carriers at related centers at these temperatures.

4 Conclusions and perspectives

The investigation performed up to now provides the evidence of the possibility to optimize the optical properties of an intrinsic scintillator as PWO, by the use of selected trivalent dopants (particularly La^{3+}) at suitable concentrations. Joined to other essential requirements in the crystal preparation, as the control of the raw material purity and of the growing methods, the introduction of trivalent dopants was found to be very successful in lowering the concentration of point defects in the lattice which strongly affect scintillation speed and radiation hardness.

The simultaneous application of different experimental techniques on selected PWO samples, undoped and intentionally doped as well, grown from high purity raw powders and supported by sophisticated chemical analyses (GDMS and ICP) of as grown crystals appeared very useful for understanding of microscopical mechanisms, which determine the scintillation characteristics and radiation resistance of PWO. At the same time, understanding of these processes could allow further optimisation of PWO scintillator characteristics, namely through described trivalent ion doping into Pb sublattice.

As the most significant results achieved can be mentioned:

- understanding of the influence of the energy transfer processes and of trivalent doping in the luminescence and scintillation decay kinetics
- revealing of correlations between observed changes in the emission decay, low temperature TSL and LY characteristics
- proposal for the microscopic radiation damage mechanism consisting in the creation of two kinds of hole centers and two kind of electron ones
- explanation of the improvement of the transmission and radiation resistance of trivalent (mostly La^{3+}) dopants, based on the coulombic compensation in Pb-sublattice and resulting in the decrease of stable and temporary hole centers in the crystal.

Future development should consists in a more systematic study of other trivalent dopants as Lu, Y and Gd, with the aim to understand possible differences in the characteristics (as e.g. that in recovery kinetics, see 3.2.5); moreover, further investigation will be devoted to the effect of Nb doping as well. According to the guidelines already followed up to now in the project, the effects of different dopants will be investigated both in the scintillation kinetics and in radiation damage mechanisms. In addition to the already used experimental techniques also electron paramagnetic resonance and wavelength resolved TSL measurements at low temperatures are planned, as useful tools to obtain significant information on the nature of electron and hole centers in the material.

References

[1] W. van Loo, Phys.stat.sol. (a) **27**, 565 (1979); **28**, 227 (1979) .
[2] R.Grasser, E.Pitt, A.Scharmann, G.Zimmerer, phys.stat.sol. (b) **69**, 359 (1979).
[3] J.A.Groening, G.Blasse, J.Sol.St.Chem. **32**, 9 (1980).
[4] R.Oeder, A.Scharmann, D.Schwabe, B.Vitt, J.Cryst.Growth **43**, 537 (1978).
[5] E.V. Tkachenko, N.A.Laishevtseva, B.V.Shulgin, V.S.Startsev, E.P.Nabereshneva, Izv.Akad.Nauk SSSR, Neorg.Mat. **24**, 1879 (1988).
[6] V.G. Baryshevski, M.Korzhik, V.I.Moroz, V.B.Pavlenko, A.F.Lobko, A.A.Fedorov, V.A.Kachanov, S.G. Solovyanov, D.N. Zadneprovskii, V.A.Nefedov, P.V.Dorogovin, L.L. Nagornaya NIM **A322**, 231 (1992).
[7] M. Kobayashi, M.Ishii, Y.Usuki, H.Yahagi, NIM **A333**, 429 (1993).
[8] P.Lecoq, I.Dafinei, E.Auffray, M.Schneegans, M.V.Korzhik, O.V.Missevitch, V.B.Pavlenko, A.A.Fedorov, A.N.Annenkov, V.L.Kostylev, V.D.Ligun, NIM **A365**, 291 (1995).
[9] M.Kobayashi, M.Ishii, K.Harada, Y.Usuki, H.Okuno, H.Shimizu, T.Yazawa, NIM **A373**, 333 (1996).
[10] R.Y.Zhu, D.A.Ma, H.B.Newman, C.L.Woody, J.A.Kierstead, S.P.Stoll, P.W.Levy, NIM **A376**, 319 (1996).
[11] D.I.Alov, N.V.Klassen, N.N.Kolesnikov, S.Z.Shmurak in: Inorganic Scintillators and their applications, ed. P.Dorenbos, C.W. van Eijk, Delft University Press 1996, p. 267 (Proc. of SCINT`95, Aug 28 - Sep 1, 1995, Delft, The Netherland).
[12] D.I. Alov, S.I.Rybchenko, Mat.Sci.Forum **239-241**, 279 (1997).
[13] J.M.Moreau, Ph.Galez, J.P.Peigneux, M.V.Korzhik, J.Alloys and Comp. **238**, 46 (1996).
[14] M.V.Korzhik in: Inorganic Scintillators and their applications, ed. P.Dorenbos, C.W. van Eijk, Delft University Press 1996, p. 241 (Proc. of SCINT`95, Aug 28 - Sep 1, 1995, Delft, The Netherland).
[15] A.N.Belski, V.V.Mikhailin, A.N.Vasiljev, I.Dafinei, P.Lecoq, C.Pedrini, P.Chevallier, P.Dhez, P.Martin, Chem.Phys.Lett. **243**, 552 (1995).
[16] G.Tamulaitis, S.Buracas, V.P.Martinov, V.D.Ryzhikov, H.H.Gutbrod, V.I.Manko, phys.stat.sol. (a) **157**, 187 (1996).
[17] K.Polak, M.Nikl, K.Nitsch, M.Kobayashi, M.Ishii, Y.Usuki, J.Lumin. **72-74**, 781 (1997).
[18] M. Nikl, K.Nitsch, K.Polak, E.Mihokova, I.Dafinei, E.Auffray, P.Lecoq, P.Reiche, R.Uecker, G.P.Pazzi, phys.stat.sol (b) **195**, 311 (1996).
[19] V.Murk, M.Nikl, E.Mihokova, K.Nitsch, J.Phys.Cond.Mat. **9**, 249 (1997).
[20] M.Martini, G.Spinolo, A.Vedda, M.Nikl, K.Nitsch, V.Hamplova, P.Fabeni, G.P.Pazzi, I.Dafinei, P.Lecoq, Chem.Phys.Lett. **260**, 418 (1996).
[21] A. Hofstaetter, R.Oeder, A.Scharmann, D.Schwabe, B.Vitt, phys.stat.sol. (b) **89**, 375 (1978).
[22] M.Springis, V.Tale, I.Tale, M.Barbosa Flores, L.L.Nagornaya, ibid. ref. 14, p. 303
[23] E.Auffray, I.Dafinei, P.Lecoq, M.Schneegans, Rad.Eff.Def. **135**, 343 (1995).
[24] M.Springis, V.Tale, I.Tale, J.Lumin. **72-74**, 784 (1997).
[25] M.Martini, E.Rosetta, G.Spinolo, A.Vedda, M.Nikl, K.Nitsch, I.Dafinei, P.Lecoq, J.Lumin. **72-74**, 689 (1997).
[26] C.Y.Chen, K.L.Sweeney, L.E.Haliburton, phys.stat.sol. (a) **81**, 253 (1984).
[27] O.F.Schirmer, D. von der Linde, Appl.Phys.Lett. **33**, 35 (1978).
[28] E.Auffray, I.Dafinei, F.Gautheron, O.Lafond-Puyet, P.Lecoq, M.Schneegans, in: Inorganic Scintillators and their applications, ed. P.Dorenbos, C.W. van Eijk, Delft University Press 1996 , p. 282 (Proc. of SCINT`95, Aug 28 - Sep 1, 1995, Delft, The Netherland).
[29] M.Nikl, K.Nitsch, J.Hybler, J.Chval, P.Reiche, phys.stat.sol. (b) **196**, K7 (1996).
[30] A.Annenkov, A.A. Fedorov, Ph. Galez, V. A. Kachanov,M. V. Korzhik, V. D. Ligun, J. M. Moreau, V.N. Nefedov, V. B. Pavlenko, J. P. Peigneux, T. N. Timoshchenko, B. A. Zadneprovskii, phys.stat.sol. (a) **156**, 493 (1996).
[31] S. Baccaro, B. Borgia, A. Cecilia, I. Dafinei, M. Diemoz, P. Fabeni, M. Nikl, M. Martini, M. Montecchi, G. Pazzi, G. Spinolo, A. Vedda, Nuclear Physics B (Proc. Suppl.) 61B (1998) 66-70.
[32] S. Baccaro, L. M. Barone, B. Borgia, F. Castelli, F. Cavallari, F. de Notaristefani, M. Diemoz, R. Faccini, A. Festinesi, E. Leonardi, E. Longo, M. Montecchi, G. Organtini, L. Pacciani, S. Pirro, NIM A 385 (1997) 69-73.
[33] M.Nikl, K. Nitsch, E. Mihokova, K. Polak, G. P. Pazzi, P. Fabeni, M. Martini, G. Spinolo, A. Vedda, V. Murk, S. Baccaro, I. Dafinei, M. Diemoz, M. Kobayashi, P. Lecoq, Proc. Of SCINT'97, Shanghai, 22-25 Sept, 1997, China, p. 171.

[34] M. Nikl, P.Strakova, K.Nitsch, K.Polak, V. Mucka, O. Jarolimek, J. Novak, P. Fabeni, "Energy transfer processes in $PbWO_4$ luminescence". Submitted to Chem.Phys.Lett.
[35] M.Nikl, P.Bohacek, K.Nitsch, E.Mihokova, M.Martini, A.Vedda, S.Croci, G.P.Pazzi, P.Fabeni, S.Baccaro, B.Borgia, I.Dafinei, M.Diemoz, G.Organtini, E.Auffray, P.Lecoq, M. Kobayashi, M.Ishii, Y.Usuki, Appl.Phys.Lett. **71**, 3755-3757, 1997.
[36] M.Nikl, J.Rosa, K.Nitsch, H.R.Asatryan, S.Baccaro, A.Cecilia, M.Montecchi, B.Borgia, I.Dafinei, M.Diemoz, P.Lecoq, Mat.Sci.Forum **239-241**, 271 (1997).
[37] G. Born, A. Hofstaetter, A. Scharmann, phys.stat.sol. **37**, 255 (1970).
[38] G. Born, R. Grasser, A. Scharmann, phys.stat.sol. **28**, 583 (1968).
[39] S.Baccaro, P.Bohácek, B.Borgia, A.Cecilia, I.Dafinei, M.Diemoz, M.Ishii, O.Jarolimek, M.Kobayashi, M.Martini, M.Montecchi, M.Nikl, K.Nitsch, Y.Usuki, A.Vedda, phys.stat.sol.(a) **160**, R5 (1997).
[40] M.Kobayashi, Y.Usuki, M.Ishii, T.Yazawa, K.Hara, M.Tanaka, M.Nikl, K.Nitsch, NIM **A399**, 261 (1997).
[41] M.Nikl, K.Nitsch, S.Baccaro, A.Cecilia, M.Montecchi, B.Borgia, I.Dafinei, M.Diemoz, M.Martini, E.Rosetta, G.Spinolo, A.Vedda, M.Kobayashi, M.Ishii, Y.Usuki, O.Jarolimek, R.Uecker, J.Appl.Phys. **82**, 5758-5762, (1997)
[42] Y.Usuki, M.Ishii, M.Kobayashi, K.Hara, M.Tanaka, M.Nikl, K.Nitsch, "Lead deficiency in single crystals of $PbWO_4$ grown in air" KEK preprint, 97-194, October 1997.
[43] Y.Zhang, W.A.N. Holzwarth, R.T. Williams, "Electronic band structures of the scheelite materials- $CaMoO_4$, $CaWO_4$, $PbMoO_4$ and $PbWO_4$" submitted to Phys.Rev.B
[44] P. Weightman, B. Henderson, D.E. Dugdale, phys. Stat. Sol. (b) 58,321 (1973)
[45] V.V. Laguta, J.Rosa, M.I. Zaritski, M.Nikl, Y.Usuki, "Polaronic WO_4^{3-} centers in $PbWO_4$ crystal", submitted to J.Phys.Cond.Mat.
[46] M.Kobayashi, Y.Usuki, M.Ishii, T.Yazawa, K.Hara, M.Tanaka, M.Nikl, S.Baccaro, A.Cecilia, M.Diemoz, I.Dafinei, NIM A404, 149-150 (1998).
[47] J. A. Groenink, H. Binsma, J. Sol. St. Chem. 29, 227 (1979).
[48] E.Auffray, P.Lecoq, M.Korzhik, A.Annenkov, O.Jarolímek, M.Nikl, S.Baccaro, A.Cecilia, M.Diemoz, I.Dafinei, NIM **A402**, 75 (1998).
[49] S. Baccaro,B. Borgia, A. Cecilia, I. Dafinei, M. Diemoz, M. Nikl, M. Montecchi,"Lead Tungstate scintillators for LHC EM-Calorimetry", accepted in Radiation Physics and Chemistry.
[50] S.Baccaro, P.Bohácek, B.Borgia, A.Cecilia, I.Dafinei, M.Diemoz, M.Ishii, O.Jarolimek, M.Kobayashi, M.Martini, S.Croci, M.Montecchi, M.Nikl, E.Mihokova, K.Nitsch, Y.Usuki, A.Vedda, Proc. of SCINT'97, 22 - 25 Sept, 1997, Shanghai, China, p. 203.
[51] S.Baccaro, P.Bohácek, B.Borgia, A.Cecilia, S.Croci, I.Dafinei, M.Diemoz, P.Fabeni, M.Ishii, M.Kobayashi, M.Martini, M.Montecchi, M.Nikl, K.Nitsch, G.Organtini, G.P.Pazzi, Y.Usuki, A.Vedda, phys.stat.sol.(a) **164**, R9 (1997).
[52] A.Cecilia, "Danneggiamento da radiazione dei cristalli di Tungstato di Piombo impiegati nella rivelazione di sciami elettromagnetici" Diploma thesis in Physics, Rome University "Tor Vergata", 1996.
[53] S. Baccaro,B. Borgia, F. Cavallari, A. Cecilia, M. Diemoz, A. Festinesi,E. Leonardi, A. Lobko, E. Longo, M. Montecchi,G. Organtini, B. Rapone, J. of Lumin., 72-74 (1997) 66-70.